THESIS

DEBRIS FLOW SUSCEPTIBILITY ANALYSIS BASED ON LANDSLIDE INVENTORY AND RUN-OUT MODELLING IN MIDDLE PART OF KODIL WATERSHED, CENTRAL JAVA, INDONESIA

Thesis submitted to the Double Degree M.Sc. Programme, Gadjah Mada University and Faculty of Geo-Information Science and Earth Observation, University of Twente in partial fulfilment of the requirement for the degree of Master of Science in Geo-Information for Spatial Planning and Risk Management

UGM **ITC**

By:
FATHIYYA ULFA
(15/389605/PMU/08564)
(6028497 – AES)

Supervisors:
1. **Prof. Dr. Junun Sartohadi, M.Sc**
2. **Prof. Dr. V.G. Jetten**

GRADUATE SCHOOL
GADJAH MADA UNIVERSITY
FACULTY OF GEO-INFORMATION AND EARTH OBSERVATION
UNIVERSITY OF TWENTE

2017

DISCLAIMER

This document describes a work undertaken as part of Double Degree International Program of Geo-information for Spatial Planning and Risk Management, a Joint Education Program of Institute for Geo-Information Science and Earth Observation, the Netherland and Gadjah Mada University, Indonesia. The author declare that this document has never been submitted to obtain a degree at any other university and does not contain the work or opinion ever written or published by others, except the writing which clearly referred as mentioned in the bibliography. All views and opinions expressed therein remain the sole responsibility of the author and do not necessarily represent both of the institutes.

Yogyakarta, April 2017

Fathiyya Ulfa

Debris flow susceptibility analysis based on landslide inventory and run-out modelling in Middle Part of Kodil Watershed, Central Java

Fathiyya Ulfa[1], Junun Sartohadi[2], Victor G. Jetten[3]

Abstract

Nowadays, flow modelling for debris flow susceptibility is commonly applied, yet there are some deficiencies faced by only using the model. Modelling process is only determined by some input factors that they capable to use as input, yet other factors which are not included in modelling parameters might give influence to debris flow occurrence. Other parameters causing debris flow must be clearly identified for intense by landslide inventories, which will determine other parameter that may not include as modelling input parameter but in fact causing debris flow occurrences. Therefore, this research is aimed to do debris flow susceptibility analysis using debris flow inventory as well as modelling. The landslide inventory was further analyzed become landslide susceptibility using weight of evidence analysis, while the modelling process was applied using RAMMS (rapid Mass movements simulations). As a result, from inventory analysis, in the study area the debris flow was commonly occurred in old andesite geological formation with plantation or paddy field as the land use then has slope around 25 to 45 % or 15 to 25% in structural landform, furthermore triggered by more than 250 mm three days cumulative rainfall. On the other hands, by modelling result, the debris flow occurred on the soil, which has high density (ρ), while low in earth pressure coefficient (λ), viscous turbulent friction (ξ), dry coulomb friction (μ) and cohesion (c). By those results, the area susceptible to debris flow can be constructed from the parameter resulted from inventory analysis while to identify the level of susceptibility, the modelling result can be implemented.

Key word: debris flow, landslide inventory, weight of evidence, RAMMS.

[1]Student of Geoinformation for Spatial Planning and Risk Management, Gadjah Mada University
[2]Faculty of Geography, Gadjah Mada University, Indonesia
[3]Faculty of Geo-information and Earth Science, University of Twente, The Netherlands

Acknowledgement

Alhamdulillahirabbil’alamin, praise to Allah SWT for the mercy and guidance, which enabled me to complete this research in order to finish my MSc course. This work is impossible to be done without the supports, contributions, helps, suggestions and comments from many people. Therefore, I would like to thanks to:

1. My parent (Ayah Aguslir and Ibu Zulfamayetti), Kak Hanna and Auliyya who support me mentally and physically not just in finishing this wok, but during the entire study program.
2. Beasiswa Unggulan, Kemendikbud for providing financial support for the course, both during in UGM and also ITC.
3. UGM supervisor, Pof. Dr. Junun Sartohadi, M.Sc as well as ITC supervisor, Prof. Dr. V. G. Jetten, who give guidance, suggestion and comment till my thesis is finished.
4. Geoinfo friends, batch 11, Geografi UI 2011, ITC colleges who give me encouragement during high and low spirit to finish this work.
5. Transbulent team who have shared their knowledge and energy during data collection.
6. Yose for the support and companion during thesis activities from starting the thesis, collecting data until finishing the writing.
7. All the influential people who could not be mentioned one by one.

Table of Contents

List of Figures

List of Tables

CHAPTER 1. INTRODUCTION

1.1 Background

Landslides are a common ground surface phenomenon on the Earth which are mostly triggered by factors that make a slope unstable, such as seismic activity, rainfall induced soil and groundwater changes and man-made activities such as road and building construction (Arnous, 2010). They are indicated as one of the natural hazards that have high losses and casualties. The high losses are determined by landslide occurrence frequency, yet individual landslides might not have high losses. Therefore, losses caused by landslide occurrence are often underestimated in the official damage estimations. To reduce economic losses caused by landslides in the future, landslide vulnerability assessments are needed.

Landslides are one of the disasters in Indonesia which bring extensive damage to properties and loss of life. In Central Java Province itself, data recorded by BNPB (n.d.) have found 109 landslides occurrence in 2016 which caused 59 casualties and much damage to properties. According to many studies that have been done in the Middle Part of Kodil Watershed, which is administratively included in Central Java Province, Rusdiyatmoko (2013) reported 152 landslide occurrence from 2003 to 2012. The landslides occurred on hilly to mountainous topography and are mostly triggered when the soil, which contains clay material, are exposed by continuous rainfall. The landslide occurrence not only impacts the source area of a landslide, but also the area downslope, the runout area. In fact, both are used for settlement and agriculture purpose. To reduce the risk of both areas, it is necessary to determine the exact area to be impacted by the landslide.

Genetically and morphologically, the area in a landslide will be divided into two zones, including the upper part where the failure is generated and the lower part which is affected by material movement from the upper part (Vescovi, 2006). Both the area are impacted during landslide occurrence.

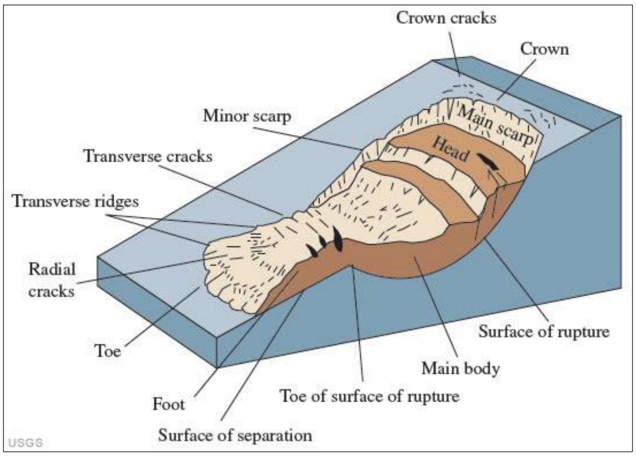

Figure 1.1. Depletion and accumulation zone
source: http://geology.com/usgs/landslides/

Varnes (1984) defined the upper part as depletion zone, while the lower part as accumulation zone. The depletion zone is the area where elevation becomes lower as an impact of the material movement. While the accumulation zone is the area which is impacted by material movement, or in other words, it is the area covered by debris. As shown in figure 1, depletion zone is the area from landslide scarp to the toe of surface of rupture, whereas accumulation zone is the area from the toe of surface of rupture until landslide toe.

The accumulation zone will be more significant on the flow-like landslides. In the flow-like landslides, fluid material will be moved on a rigid bed

(Hungr et al., 2001). As a result of its motion, landslides with long run-out will occur. Accumulation zone might be placed on the area which might be far from the source area.

From the 152 landslide occurrences in the Middle Part of the Kodil Watershed, generally the landslide types are slide and slump. Around 8 landslides of total landslides have more than 100 m run-out distance which will not be classified as slide neither or slump. These types of landslide can be classified as debris flow. This study will try to discover the reason of debris flow occurrence among other different type of landslide such as slide and slump.

1.2 Research Problem

Regarding landslide susceptibility assessment, many researchers have focused on the study of the depletion zone (source area), yet susceptibility assessments focusing on potential accumulation zones (area covered by landslide material) is limited. For instance, Arnous (2010) and Feizizadeh et al. (2014) used remote sensing and geographic information systems to estimate landslide susceptible area. The research emphasized the prediction of landslide triggering areas, but did not discuss areas prone to coverage by landslide material. Meanwhile, as described in Quan Luna et al. (2013) and Blahut et al. (2013), the accumulation zone has higher risk than depletion zone, because the bottom of slopes is usually more densely populated than the upper part.

Flow modelling studies are being done to predict potential accumulation zone of future events (Schraml et al., 2015). Flow-like modelling studies can be applied to reduce property damage and loss caused by the flow of landslide material. Moreover, flow-like modelling studies could give a precise prediction of runout distance and velocity, which can be used as hazard intensity estimation for risk studies and protective measures (Cesca & D'Agostino, 2008).

Flow-like landslide modelling is considered as a relatively new research. Guo et al. (2014) used historical landslide events to build a model in evaluating landslide travel distance. Besides, 2-dimensional models have been applied such as FLOW-R which delimits run-out areas based on multiple flow direction and energy based algorithm which only used DEM as a parameter (J. Blahut et al., 2010). Another research used 2-dimensional model named FLO-2D to simulate debris-flow by using shear stress characteristic based on laboratory analysis as the input parameter (Quan Luna et al., 2013).

Besides, flow-like landslide modelling could also be done by using dynamic models. One of the examples is dynamic model DAN3D which uses rheology rules, friction angle and Voellmy fluid assumption as parameters (Zhang et al., 2013). Then another example is RAMMS which uses DEM, release area and friction parameters as input data (Christen et al., 2012).

From the researches that have already been done, it can be concluded that different model requires different input parameters that will influence the result. In reality, run-out occurrences are not only influenced by the model parameters itself, but also is influenced by other factors. For example, RAMMS needs DEM, soil parameter, and landslide volume as input parameters. In fact, other factors, like rainfall and landform, in a particular area might play important roles. To obtain a proper result, the modelling process should be followed by landslide inventory that considered other specific factors triggering landslide run-out. Thus, this research is aimed to combine flow modelling with landslide inventory analysis to get specific factors causing flow-like landslide. Then, by those parameters, flow-like landslide susceptibility analysis will be properly matched to the study area. Finally, this kind of flow-like landslide susceptibility analysis will be effective to reduce the impact caused by landslides.

1.3 Goal and Objectives

Goal

The main objective of this research is to analyse debris flow susceptibility based on landslide inventory and model calibration in the Middle Part of Kodil Watershed.

Specific objectives

a. To identify updated landslide susceptibility in the Middle Part of Kodil Watershed.
b. To analyze and model debris flow behavior in the Middle Part of Kodil Watershed.
c. To combine landslide susceptibility parameter and calibrated model input parameter on debris flow susceptibility area identification.

1.4 Research Questions

Table 1.1. Objectives and research questions

No	Objectives	Research Questions
1	To identify landslide susceptibility in the Middle Part of Kodil Watershed.	a. How to build a landslide susceptibility map? b. How landslide inventory influence landslide susceptibility? c. Which class of the landslide parameters are causing the debris flow?
2	To analyze debris flow behavior in the Middle Part of Kodil Watershed.	a. What are debris flow characteristics in previous events? (e.g. debris flow duration, height, and volume) b. Based on debris flow modelling, how input parameter influence the debris flows?
3	To combine landslide susceptibility parameter and calibrated model input parameter on debris flow susceptibility identification.	a. Which parameters can be used to determine the susceptible area to debris flow and the level of debris flow susceptibility? b. Can improved parameters be used to generate a debris flow susceptibility map?

1.5 Thesis Structure

This thesis has the following structure:
Chapter 1 introduces the study background stating why the research is being done, then followed by research objectives and questions.

Chapter 2 is literature review describing landslide in general, debris flow, and debris flow assessment using landslide susceptibility information and debris flow modelling.

Chapter 3 explains the materials needed in the research as well as the method used to collect and process the materials.

Chapter 4 describes the study area condition including physical and social aspects of the area.

Chapter 5 is result and discussion of the study including landslide assessment, debris flow modelling and debris flow assessment.

Chapter 6 is final conclusion which states the objective achievement and the recommendation for the study area itself as well as the future studies.

CHAPTER 2. LITERATURE REVIEW

2.1 Landslides

Mass movement processes are commonly simplify with term landslides. In fact, the landslides can be differentiated into several types based on their material types and movement types. The material types are classified as rock, soil, earth, mud, debris, while the movement types including fall, topple, slide, spread and flow (Varnes, 1978).

Table 2.1. Mass movement classification of Varnes (1978)

Type of Movement		**Type of Material**		
		Bedrock	**Engineering Soils**	
			Predominantly Coarse	**Predominantly Fine**
Falls		Rock fall	Debris fall	Earth fall
Topples		Rock topple	Debris topple	Earth
Slide	**Rotational**	Rock slump	Debris slump	Earth slump
	Translational	Rock block slide	Debris block slide	Earth block slide
		Rock slide	Debris slide	Earth slide
Lateral Spreads		Rock spread	Debris spread	Earth spread
Flows		Rock flow	Debris flow	Earth flow
		Deep creep	Soil Creep	
Complex (combination of two or more principal types of movement)				

2.2 Debris Flows

Many researchers have their own definition of debris flow, which has been updated over the years. Varnes (1978) defined debris flow as the flow-like landslide which is distinguished by the high percentage of coarse particle. Commonly it is triggered by unusual heavy precipitation, which caused torrential runoff on steep slopes and caused a rapid flow on preexisting drainage ways. Varnes (1978) also mentioned that debris flow will be triggered by a certain rate and durations of rainfall, physical properties of material and deposit, slope angle, pore-water pressure, and movement mechanism. Besides, Hungr et al. (2001) described that debris flow occurs when the water content of debris material is saturated, which caused rapid velocity of movement on a regular confined path. According to his research, debris flow velocity excess 1m/s up to 10m/s.

In 2007, Sassa et al. defined debris flow as a mixture of water and sediment which flow down as if it continuous fluid. According to (Sassa et al., 2007), debris flows are initiated because three predominant causes. The first cause is due to channel bed erosion, which is triggered by a severe rainfall. The second cause is due to a landslide which lead material movement. And the other cause is destruction of natural dam on the upper part of the slope.

Debris flow can be divided into two different classifications, they are hillslope debris flow or known as open-slope debris flow and channelized debris flow. These two classifications are made based on topographic and geological characteristic of the location where the debris flow placed. Hillslope type of debris flow forms its own path down the slope, while channelized type flows on the existing pathway for instance rivers, gullies, valleys or depressions. (Nettleton et al., 2005)

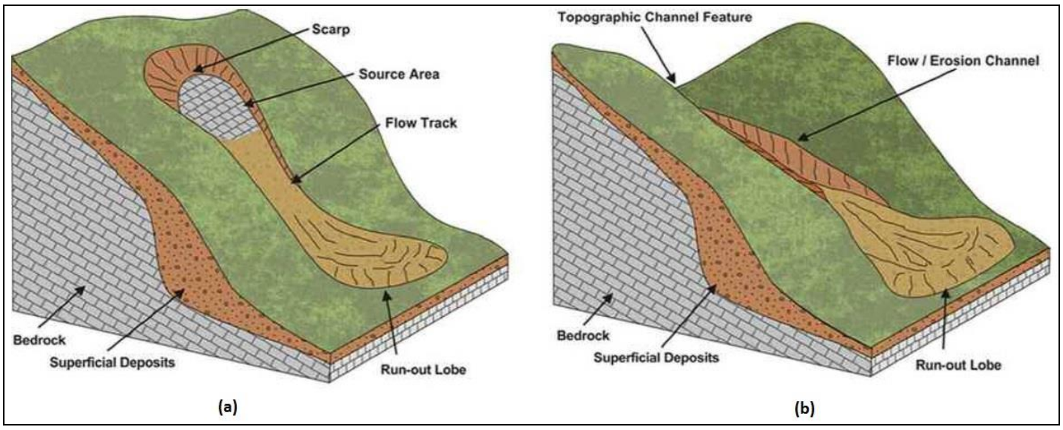

Figure 2.1. Hillslope debris flow (left) and Channelized debris flow (right)

2.3 Landslide Inventory

Landslide inventory is an inventory of the location, classification, volume, activity, date of occurrence and other characteristic of landslide in an area (Fell et al., 2008). In a simple word, landslide inventory is recorded data about past landslides distribution and characteristic. Complete landslide inventory consists of coordinate, address, type, date of occurrence, extent area, dimension, geology, land use, triggering factor an causalities (Hervas, 2013). Besides, illustration, map and aerial photo could be complementary data in inventory.

Due to difficulties for data collecting, only partial data could be available in landslide inventory. All those data can be collected by aerial photo, field survey, and interviews. Commonly, the inventory will be formed as landslide distribution maps which has attribute table that contain the landslide additional information and its characteristic. Detail inventory might be applied in large landslide such as landslide source area, scrap, landslide body, and ponds. The inventory is valuable for future research, planning, and decision-making, moreover, it will be useful as basic data for landslide density, hazard, susceptibility, and risk map which essential for risk reduction measurements. (Hervas, 2013)

2.4 Landslide Susceptibility Assessment

According to Fell et al., (2008), landslide susceptibility is an assessment using qualitative or quantitative approach which determines classification, area, and spatial distribution of landslide. The landslides that are used as objects of assessment can be the landslides that already exist or potentially may occur in an area. It is expected that the more susceptible the area to landslides, the more the landslide will occur in that area. It is different from landslide hazard which took landslide frequency in a given period into account, the landslide susceptibility does not give the frequency or time frame of landslide occurrence, however it only determines the possible location of landslide occurrence.

As mention previously, landslide susceptibility assessment could be done using qualitative and quantitative approach. The qualitative approach is a method which uses knowledge driven to extract the parameter of susceptibility. Some examples of qualitative approach are fuzzy, multiclass overlay, and spatial multi criteria evaluation. Besides, quantitative approach is a method which based on data driven, some examples are bivariate statistics, weight of evidence, frequency ratio, cluster analysis and so on. Both qualitative and quantitative approaches can be used based on data availability, for instance, qualitative approach is commonly used in some countries which does not have appropriate quantitative data for landslide susceptibility assessment. (Fell et al., 2008)

This research applied quantitative approach, namely the weight of evidence analysis, which statistically calculate the importance of influential factors to the landslide occurrence. According to Song, et al. (2008), the weight of evidence is the method which usually predicts the occurrence of events based on the training data on the known fact or influential factors. By this definition, it can be concluded that the landslide inventory is the crucial data to be used in landslide susceptibility analysis using weight of evidence analysis.

2.5 Debris Flow Susceptibility Assessment

Debris flow susceptibility assessment is a part of the landslide susceptibility assessment which include both recognition of landslide source area or commonly called initiation area and landslide runout (Mandaglio et al., 2016). The landslide runout which is determined in the debris flow susceptibility assessment may consist of travel distance, velocity and intensity of existing or potential debris flow.

Debris flow modelling is one of the methods to assess debris flow susceptibility which will predict the area will be affected by hazard in future event and understand their behavior (Hussin, 2011). There are 3 categories of debris flow modelling including physical, empirical and dynamic modelling (Chen & Lee, 2004). Physical modeling is the method that conducted by field observation and further analyze the flow by laboratory analysis. In fact, it is difficult to conduct field observation for debris flows, therefore many methods are used to simplify the field observation, such as using high-speed photography or runout videotape as a controlled field (Chen & Lee, 2004).

The empirical modeling is usually based on well documented field observation (Quan Luna et al., 2013). The modelling parameters, which are collected from well documented field observation, are used for analysis by determining the relationships between each of the parameters. For instance, the relationships between runout extent area with volume of the debris flow. The input parameter for empirical model are volume estimation, topographic profiles, image interpretation, and geomorphologic studies.

The last category of the debris flow model is dynamic models which use numerical method to analyze the flow (Hussin, 2011). It is divided into 3 types including lumped mass models, distinct element models and continuum models (Chen & Lee, 2004). The lumped mass model defines debris flow as one uniformly spread out sheets, with excess pore water pressure caused by liquefaction. The district element model defines flow as a group of blocks which are analyzed using an equation based on the contact between blocks. Then, the continuum model uses rheological formula to simulate debris flow and to identify its characteristic.

This study applied dynamic continuum model by using RAMMS software which uses Voellmy rheology to identify the debris flow. RAMMS software has three input parameters including digital elevation model, release area and friction (Cesca & D'Agostino, 2008). Digital elevation model plays an important role for run-out simulation since it will determine run-out volume in the initiation part and also determine the visualization of the model. Another parameter is release area which need to be identified to know the source of debris flow and how much the volume of landslide run-out. To determine run-out volume, release area should be followed by release height information. Then the last parameter, friction parameter, consist of two data, including viscous turbulent friction (ξ) and dry coulomb friction friction (μ) (Bartelt et al., 2010). The viscous turbulent friction (ξ) controls the velocity of the flow, which is determined by the type of flow material whether it granular or muddy material. While the dry coulomb friction (μ) controls when the flow will stop which is determined from the tangent value of slope angle in the deposition zone. Furthermore, deposit extent, velocity, flow depth and impact pressures will be the outputs of the model (Quan Luna, 2012).

2.6 Theoretical Framework

In this research, debris flow susceptibility analysis is determined by two analysis, including landslide susceptibility in general and debris flow modelling. Both processes are applied to define specific parameter which cause debris flow occurrence. Landslide susceptibility analysis is obtained using weight of evidence analysis of several parameters which will be visualized on factor maps. Since the weight of evidence analysis depends on landslide density, landslide inventory should be done earlier. Beside using landslide inventory for landslide susceptibility determination, it is also used for defining the type of landslide, whether they are categorized as debris flow or other types. Further, it will be used for determining specific parameter that will cause the debris flow type.

The specific parameters causing debris flow, which have been determined using the landslide susceptibility analysis will be improved by debris flow modelling. To run the model, back analysis method is applied in several debris flow events. Then calibration is applied using the extent area which is obtained from aerial photos. From debris flow modelling, specific parameter causing debris flow will be obtained. The specific parameters, resulted both from landslide susceptibility analysis and debris flow modelling, are integrated to determine debris flow susceptibility.

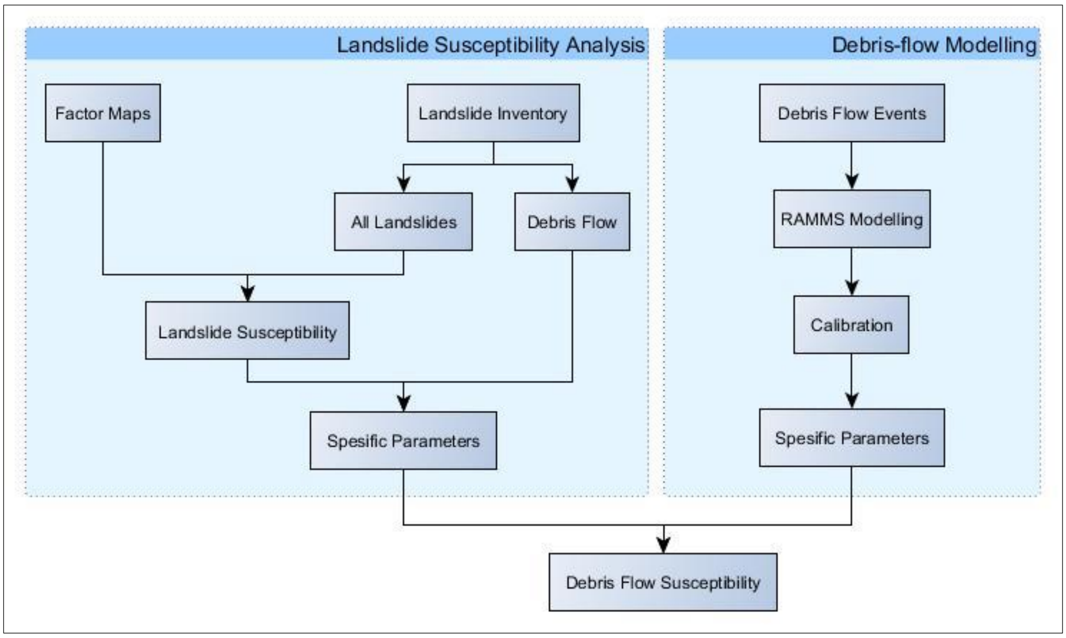

Figure 2.2. Theoretical framework

CHAPTER 3. MATERIALS AND METHODS

3.1 Materials and Equipment

There are several data needed in this research:

a. Landslide data

Landslide data were needed to determine landslide density, which further were used in landslide susceptibility analysis. These data were collected from previous research, governmental institution and participatory mapping. The data from previous research were consist of landslide data from 2003 until 2012, while 2013 until recent data were collected from governmental institutions such as BPBD Magelang and Purworejo Regency. Moreover, the participatory mapping from village officers was held to determine the exact coordinate of recorded landslide data from the governmental institutions.

b. Rainfall

Daily rainfall data from 2006 to 2015 were collected from 6 stations surrounding the study area, then furthermore were used to determine landslide susceptibility. The rainfall data were obtained from a governmental institution, namely BPSDA (Balai Pusat Sumber Daya Air) Probolo.

c. Topographic data

Topographic data were needed to extract slope information of the study area. It was generated from 9 m resolution Terrasar DEM which was obtained from a governmental institution, namely BIG (Badan Informasi Geospatial).

d. Geological map

Geological map was obtained from the Geological Map of The Yogyakarta Sheet 1977 which was established by the Geological Survey of Indonesia. It was used as one of parameters determining the landslide susceptibility.

e. High resolution image

There were 2 main purposes of high resolution imagery for the research, including geomorphological map extraction and landslide inventory determination. As same as topographic data, high resolution imagery was also obtained from BIG. The high resolution imagery used was the Pleiades image year 2015 with 0,5 m pixel resolution.

f. Land use

Land use data were obtained from online resource of BIG under tanahair.indonesia.go.id website. The data were extracted from Rupa Bumi Indonesia Map which produced by BIG at scale 1:25.000. The data were also used as one of parameters to determine landslide susceptibility.

g. Aerial Photograph

Aerial photograph, which was used for modelling input parameter and visualization, was obtained from data acquisition using drone namely DJI Phantom 4. Furthermore, photos that were captured by drone camera was compiled become a mosaic using Agisoft software.

h. Soil properties

Soil properties were taken from laboratory analysis of soil samples by two kinds of analysis, including grain size distribution and plasticity index analysis. The result of the analysis was the type of soil which determined the model input parameters such as soil density (ρ), earth pressure coefficient (λ), viscous turbulent friction (ξ), dry coulomb friction (μ) and cohesion (c).

Some software were used in research analysis including;

Table 3.1. Software used in the research

No	Software	Version	Function
1	ArcGIS	10.1	GIS processing
2	Ilwis	3.4	Weight of evidence analysis
4	Agisoft	1.2	Compiling aerial photos
5	RAMMS	1.5	Debris flow modelling
6	Ms. Word	2013	Word processing
7	Ms. Excel	2013	Spreadsheet processing
8	Ms. Power Point	2013	Presentation

Beside software, there are some equipment used for data acquisition, they are;

Table 3.2. Equipment used in the research

No	Equipment	Function
1	DJI Phantom 4	Aerial photo acquisition
2	Sieves	Soil laboratory analysis
4	Casa Grande	Soil laboratory analysis

3.2 Method Applied

3.2.1 Analyzing Landslide Susceptibility

In this research, landslide susceptibility analysis was used for determining the parameters and their classification which cause a debris flow. The landslide susceptibility analysis was determined using data driven method, namely the weight of evidence analysis, which was proceed using Ilwis 3.4. Generally, the weight of evidence method assessed the relationship between the distribution of landslide occurrence and the distribution of the parameter causing landslide (Barbieri &

Cambuli, 2009). Therefore, the first step in this analysis was generating a landslide distribution map which was based on landslide recorded data. Then in the next step, landslide parameters, such as land use, rainfall, geology, combination of slope and landform, were also generated which were further visualized into factor maps.

Aside from landslide susceptibility map, other outputs of this analysis was the weight of each class in every parameters. The weights were calculated based on the presence and absence of landslide events in each class of the parameters (Song et al., 2008). The calculated weight consists of positive weight to indicate the importance of the factor map presence for the landslide occurrence and negative weight to indicate the importance of factor map absence for the landslide occurrence (Barbieri & Cambuli, 2009). To calculate the weight of each class, the landslides distribution map was overlaid with each factor map, which further resulting four pixel combinations (Van Westen, 2002). They are;

Table 3.3. Four pixel combinations of landslides and class of parameter

		Certain class of parameter	
		Present	Absent
Landslide	Present	$Npix_1$	$Npix_2$
	Absent	$Npix_3$	$Npix_4$

Where,

$Npix_1$ = number of pixels with landslides in the class

$Npix_2$ = number of pixels with landslides outside the class

$Npix_3$ = number of pixels without landslides in the class

$Npix_4$ = number of pixels without landslides outside the class

Those combinations was used to determine positive and negative weight under the equation;

$$W_i^+ = log_e \frac{\frac{Npix_1}{Npix_1+Npix_2}}{\frac{Npix_3}{Npix_3+Npix_4}} \quad \text{and} \quad W_i^- = log_e \frac{\frac{Npix_2}{Npix_1+Npix_2}}{\frac{Npix_4}{Npix_3+Npix_4}}$$

After positive and negative weight was determined, final weights of each classes was defined using following equation;

$$W_{map} = W_{plus} + W_{\min total} - W_{min}$$

In which W min total was the total negative weights in other classes.

Finally, all weight maps was summed up to obtain landslide susceptibility map then was classified into high, moderate and low susceptibility. (Van Westen, 2002)

3.2.2 Debris Flow Modelling

Debris flow modelling was done using RAMSS software. Generally, there are two sequential steps in this modeling, including input preparation and running calculation (Bartelt et al., 2010). The input preparation is a step to prepare several data such as DEM, map and orthophoto, so that they can be used for the model interfaced. In this process, project directory was set to select the certain folder where the project was located. Subsequently, to build a model interface, project wizard was created, then the data that have been stored previously will be visualized into a three dimensional model (Christen et al., 2012).

After a model interface has been built, debris flow modelling was calculated by running calculation process. In this step, project domain, release area, and some parameters was set (Bartelt et al., 2010). The project domain is the model boundary which was determined by digitizing on the model interface. While the release area is the source boundary which was also determined by digitizing on the model interface, but additionally should contain release height information to estimate landslide volume.

Regarding the parameters, there are 2 kinds of parameters which was determined before model calculation including simulation parameters and friction parameters (Bartelt et al., 2010). The simulation parameters are simulation grid resolution, end times, dump steps, soil density (ρ) and earth pressure coefficient (λ). While friction parameters are viscous turbulent friction (ξ), dry coulomb friction (μ), and cohesion (c).

The grid resolution, the end times and the dump step are given value by the user which determined the resolution of the model result and the calculation process duration (Bartelt et al., 2010). The grid resolution is an important feature which further determines the resolution of terrain model of the simulation. Then, the end times is the maximum duration for the simulation. The proper simulation is the simulation which does not reach the end time of simulation. Moreover, the dump step is the time interval of simulation which represent the time resolution of the simulation.

Then, another simulation parameter is the soil density (ρ), which represents the ratio between the mass of soil bulk and the volume of soil, including the pore spaces (Black & Blake, 1965). The density (ρ) was determined from the soil type in the area, the following table is the typical value of soil density (Subramanian, 2008);

Table 3.4. Typical mass densities of basic soil types

Type of Soil	**Mass density (Mg/m^3)**			
	Poorly graded soil		**Well-graded soil**	
	Range	**Typical value**	**Range**	**Typical value**
Loose sand	1,70-1,90	1,75	1,75-2,00	1,85
Dense sand	1,90-2,10	2,07	2,00-2,20	2,10
Soft clay	1,60-1,90	1,75	1,60-1,90	1,75
Stiff clay	1,90-2,25	2,00	1,90-2,25	2,07
Silty soils	1,60-2,00	1,75	1,60-2,00	1,75
Gravelly soils	1,99-2,25	2,07	2,00-2,30	2,15

The last parameter in the simulation parameters is the earth pressure coefficient (λ), which represents the ratio of vertical and normal stress. It is an important parameter because it regulates the flow height of the simulation (Christen et al., 2010). This parameter was determined from the following equation (Terzaghi, 1943) ;

$$K_{a/p} = tan^2 \left(45° - \frac{\varphi}{2}\right)$$

Where, $K_{a/p}$ = earth pressure coefficient

φ = angle of friction

Aside from simulation parameters, friction parameters are also needed as input parameters in RAMMS including viscous turbulent friction (ξ), dry coulomb friction (μ), and cohesion (c) (Bartelt et al., 2010). The viscous turbulent friction (ξ) is the parameter which dominates when the flow is running quickly. It is determined by the types of flow whether granular which is represented by 100 to

200 values or mud flow which is represented by 200 to 1000 values. Then, dry coulomb friction (μ) is the parameter which dominates when the flow is close to stop or in the other words, is the normal stress at the base of the flow (Scheuner et al., 2011). It was determined from the tangential value of the soil friction angle. And the last parameter is the cohesion (c) which is the force that binds the soil particle together or in other words, it is the bond between the soil particle (Terzaghi, 1943). The cohesion (c) was determined using the typical value of a certain soil type.

From the descriptions, it can be concluded that almost all the parameters, such as soil density (ρ), earth pressure coefficient (λ), viscous turbulent friction (ξ), dry coulomb friction (μ) and cohesion (c), are determined based on the soil type in the area. Therefore, this research tries to determine the type of soil in each modelled debris flow event based on the Unified Soil Classification System (USCS). The following table consist of USCS, its friction angle and the cohesion (c);

Table 3.5. Unified Soil Classification System

No	USCS Soil Class	Description	Angle of Friction	Cohesion
1	GW	Well graded gravel	33-40	0
2	GP	Poorly graded gravel	32-44	0
3	GM	Silty gravel	30-40	0
4	GC	Clayey gravel	28-34	0
5	GW-GM or GP-GM	Silty gravel with many fines	35	0
6	GW-GC or GP-GC	Clayey gravel with many fines	29	3
7	SW	Well graded sand	33-43	0
8	SP	Poorly graded sand	30-39	0
9	SM	Silty sand	32-35	0
10	SC	Clayey sand	30-40	0

11	SW-SM or SP-SM	Silty sand with many fines	27-33	0
12	SW-SC or SP-SC	Clayey sand with many fines	31	5
13	ML	Silt	27-41	0
14	CL	Low plasticity clay	27-35	20
15	CH	High plasticity clay	17-31	25
16	OL	Organic silt	22-32	10
17	OH	Organic clay	17-35	10
18	MH	High plasticity silt	23-33	5

source: www.geotechdata.info

After the modelling process and result analysis were already done, the debris flow extent, which was produced from the model, was compared to the extent of previous event. The parameters were adjusted during the calibration process. As a result, the specific parameters causing debris flow was determined and finally are able to use for analysing debris flow susceptibility.

3.2.3 Critical Analysis of Debris flow Susceptibility

Debris flow susceptibility analysis was determined by integrating landslide susceptibility analysis and debris flow modelling which both resulting specific parameters causing the debris flow. The specific parameters produced from landslide susceptibility analysis were improved by specific parameter produced by debris flow modelling.

From landslide susceptibility analysis, a specific class of each parameter causing debris flow was produced as well as its weight to landslide susceptibility. Critical analysis was done to identify either the class of the parameter and its weight causes debris flow or not. Besides, from debris flow modelling, specific parameters formed as specific local circumstances causing debris flow was also produced. As same as landslide susceptibility analysis, the result of modelling was also critically identified.

After those critical analysis was integrated to determine the parameters of debris flow susceptibility, the integrated debris flow susceptibility was compared to the susceptibility analysis of all landslide in phase one. The comparison was aimed to know whether improved debris flow susceptibility was linear to landslide susceptibility in general or not.

3.3 Fieldwork

The fieldwork consist of 3 main activities including landslide inventory process, debris flow identification and soil sample taking. Beside collecting secondary data of landslide occurrence from institutions, the landslide inventory was also done by participatory mapping technique. According to Chambers (2006), participatory mapping is a participatory method based on local people's abilities to build geographic information. Therefore, this research involved the local authorities, such as head, secretary and staff of village offices to mark the landslide points based as well as landslide dimension identification.

Based on landslide inventory, landslide with more than 100 meter lengths, which further was called debris flow, was visited to identify whether it was suitable to be modeled or not. The debris flow was photographed by drone namely Phantom DJI 4 to obtain aerial photograph. It was used in the modelling process and was used to identify deep information of the terrain and physical analysis of the area, including landslide extent, source area and the height of the source area, so the model results were easier to interpret (Christen et al., 2008).

There are some parameters required for debris flow modelling. Commonly, the parameters can be prescribed from numerical solution or automated procedures using terrain analysis in GIS (Christen et al., 2008). Unlikely, in this research, the parameters were acquired from soil sample analysis. The soil samples were also taken to get soil property information from 3 samples of selected debris flow and 3 samples of other landslides with small dimension. The sample of small landslides was used as comparative samples to those in the selected debris flow. Furthermore, the soil samples were analyzed in a laboratory to obtain the soil type information then further determined the value of model input parameters.

3.4 Data Collection and Processing

3.4.1 Extracting 3 Days Cumulative Rainfall Data

Based on the research that have been done by Peres & Cancelliere (2014), by using a method called power-law rainfall intensity-duration, the hillslope showed the good stability when there is no continuous rainfall more than 3 days, or in other words, 3 days cumulative rainfall is the threshold for hillslope instability. Referring to the research result of Peres & Cancelliere (2014), this research was also used 3 days cumulative rainfall to assess landslide susceptibility. The data were extracted from daily rainfall data starting from 2009 to 2015 in 7 rainfall stations.

The 3 days cumulative rainfall were calculated in each day by adding the current daily rainfall with rainfall data of 2 days before. After those rainfall data were accumulated, the maximum 3 days cumulative rainfall was used as a representative value of each rainfall station. To get spatial data of 3 days cumulative rainfall, the representative values of each station were interpolated. The interpolation process was processed in ArcGIS 10.1 by using inverse distance weighted tool, which interpolated the data proportionally based on the distance between one station to others (Mair & Fares, 2011). As a result, a distribution map of 3 days cumulative rainfall was extracted and can be used as one of the parameters for landslide susceptibility analysis.

3.4.2 Extracting Landform Map

The landform map was constructed from three main inputs, including Pleiades imagery, geological map and Terrasar imagery which was used to construct a hill shade map. Imagery interpretation was applied from those 3 kind of data to generate landform classification. Interpreting landform from imagery requires key interpretation features including image tone or color, shape, shadow, association and texture (Martha, 2012).

The hill shade helps to interpret the morphology of the area by using key interpretation features such as shape, tone, and texture. The hill shade, which visualized the terrain of the area, is the important component of landform identification (Martha, 2012). It helps to know either it is generally flat which was interpreted as denudational landform, or consist of a clear dip and strike which was interpreted as structural landform, or consist of steep slopes which was interpreted as volcanic landform. On the other hands, interpreting from high resolution imagery is applied using almost all key interpretations such as color, shape, association and texture. It helps to identify the drainage pattern and vegetation condition which are useful landform interpretation. For instance, as a result from the erosion process, denudational landform has many drainage lines which closely located, nor the structural and volcanic landform. Furthermore, the lithology or soil, which was represented by geological map also helps the interpretation to know which lithological type are dominant in a certain landform unit.

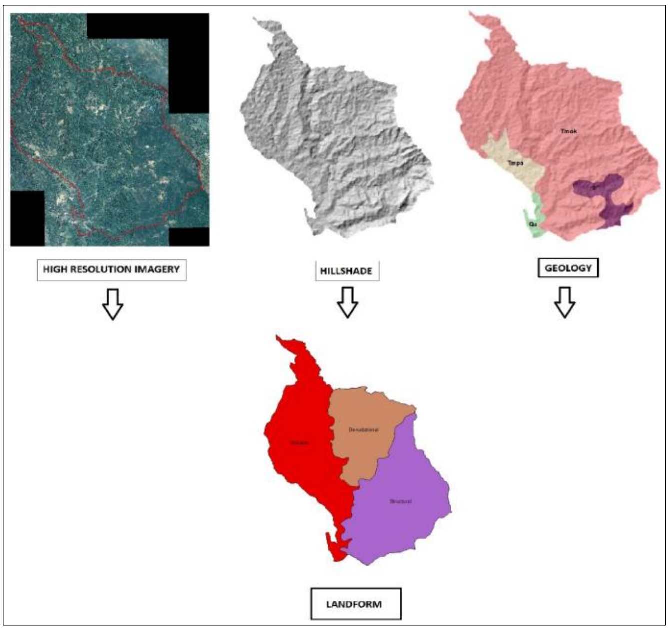

Figure 3.1. Landform construction

3.4.3 Generating Landslides Polygon

The landslides point was extracted into polygon using ArcGIS 10.1 to obtain a landslide density map which was used to assess landslide susceptibility. There are some input data for generating the landslide polygons, including landslide inventory, high resolution imagery namely Pleiades and hill shade which was extracted from Terrasar imagery. The landslide inventory, which have been recorded from local authorities, consists of the landslide dimension data which help the polygon extraction. The landslide polygons are digitized on the high resolution imagery based on possible interpretations of the landslide location from the high resolution imagery itself and also the hill shade. The high resolution imagery was used to estimate the exact area of landslide which was described in landslide inventory, while hill shade was used to estimate landslide direction.

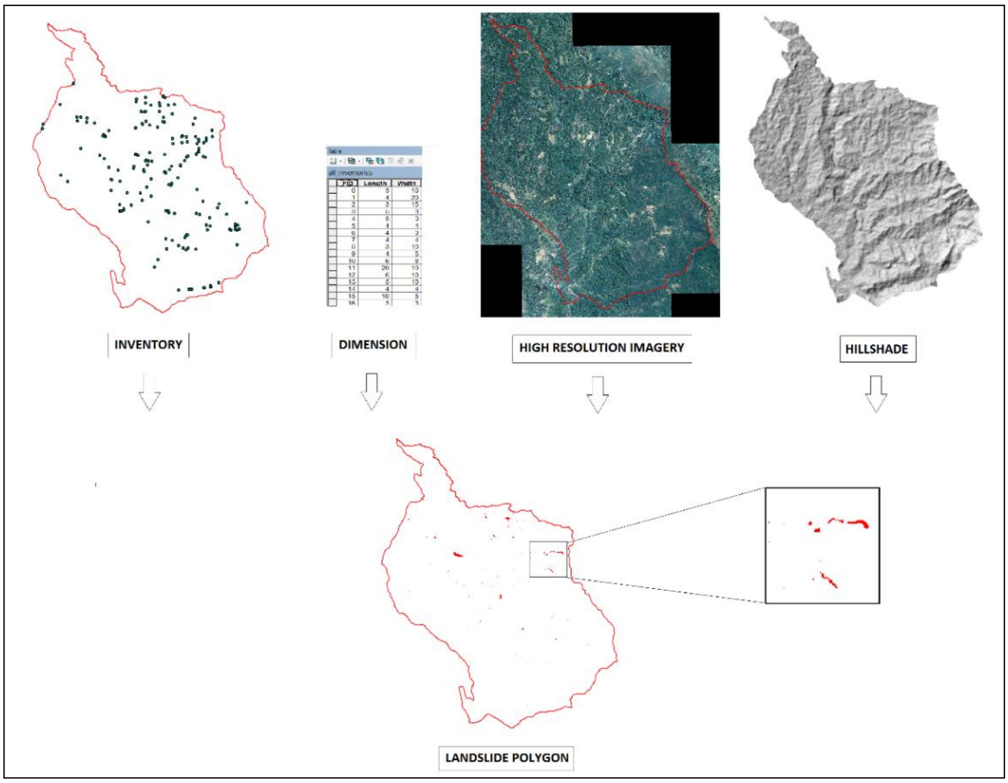

Figure 3.2. Landslide polygon construction

3.4.4 Aerial Photograph Acquisition and Photos Processing

The aerial photo acquisition was obtained using an unmanned aerial vehicle called DJI Phantom version 4 and was operated using Pix4D application which was open on PC platform. Technically, DJI Phantom was controlled by Pix4D application. Here are the sequences of aerial photo acquisition using DJI Phantom 4 and Pix4D (*Phantom 4 - user manual*, 2016):

a. UAV track, which further called as mission, was created in Pix4D application. Mission grid extent was adjusted with the total area extent to be captured, flight height, and the flight duration.
b. Flight setting was adjusted in Pix4D to control the camera angle, output photos overlap, and UAV speed.
c. The UAV was connected to Pix4D application until the mission was able to be run.
d. After all setting were set, the UAV was taken off to capture the aerial photo.

After all captured aerial photos are collected, those photos were combined to be one single mosaic so the imagery can be used in this research. The following steps are the sequences of combining photos to be single mosaic using Agisoft 1.1 (*Agisoft photoscan user manual*, 2011).

a. Importing photos. All captured photos were added to agisoft software.
b. Photos alignment. Photos alignment was done for creating points cloud which are the points connected from one photo to another.

c. Creating dense cloud. Dense cloud is point could expansion, so that many control points was generated.
d. Building mesh. It was a 3D polygonal mesh representing the object surface based on dense cloud created previously.
e. Building texture. It was the final step to build orthophoto mosaic which already consist of 3D photos, not just 3D polygonal as the previous step.

3.4.5 Laboratory Analysis of Soil

Soil laboratory analysis was used to classify the soil type based on Unified Soil Classification System (USCS) which further used to determine some parameters in modelling including soil density (ρ), earth pressure coefficient (λ), viscous turbulent friction (ξ), dry coulomb friction (μ) and cohesion (c). USCS use soil gradation information and plasticity index to classify the soil type based on the following steps (Ishibashi & Hazarika, 2011).

a. The soil was sieved using several sieves with different opening size between 0,075 mm (no. 200) and 4,75 mm (no.4) size. The soil, which finer than 0,075 further was called F200, while the soil which retain in 0,075 sieve namely R200. This naming is applied to all sieves.
b. After the sieves analysis was done, the grain size distribution was visualized in a curve then coefficient of uniformity (Cu) and coefficient of gradation (Cg) was calculated. It was used to identify whether the soil is classified as well graded or poorly graded soil.

c. For some soil classes, plasticity index was tested. Plasticity index is used to determine if the soil consists of clay or silt particle. The laboratory equipment in this test is *Casa Grande*.

The following chart is USCS flowchart to easier the classification;

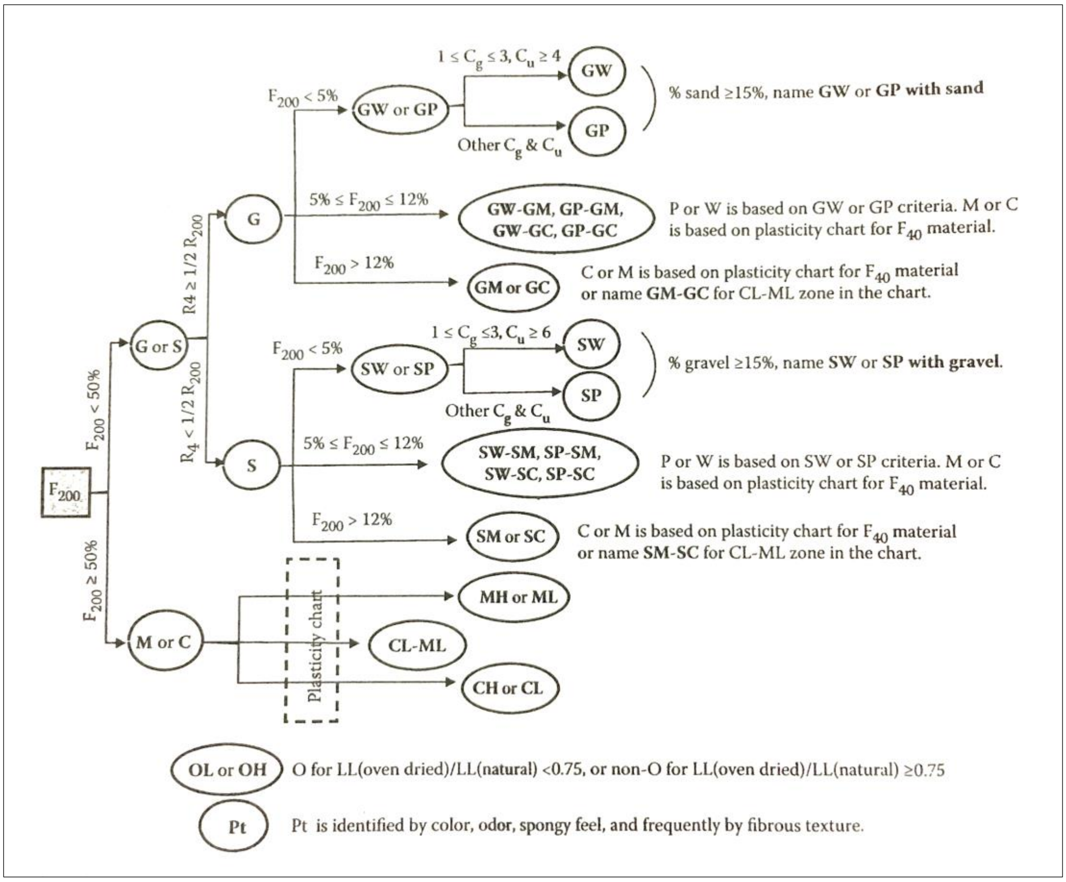

Figure 3.3. USCS flowchart

CHAPTER 4. STUDY AREA

4.1 Administrative and Geographic Position

Kodil watershed is a sub-watershed of Bogowonto which is one of the watershed located in Central Java, Indonesia. This study took place in the middle part of Kodil watershed, which specifically located in two different sub-districts, Bener sub-district belongs to Purworejo and Salaman sub district belongs to Magelang. Specifically, there are 21 villages which included in the study area, 20 of them is administratively located in Purworejo district, while the other one is located in Magelang district.

Table 4.1. Administration boundary of study area

No	District	Sub-district	Villages	
1	Purworejo	Bener	Bener	Legetan
			Bleber	Limbangan
			Cacaban Lor	Mayungsari
			Jati	Medono
			Kaliijambe	Ngasinan
			Kalitapas	Nglaris
			Kaliwader	Pekacangan
			Kamijoro	Sidomukti
			Kedungloteng	Sukowuwuh
			Ketosari	Wadas
2	Magelang	Salaman	Margoyoso	

The study only focused in the middle part because the variety of geomorphological processes, including volcanic, denudational and structural which may lead to problem focused by the study namely debris flow. Geographically, it is located between 392099,226 E – 403179,265 E and 9153946,066 N – 9167566,5399 N with 7951,18 Ha total area extent.

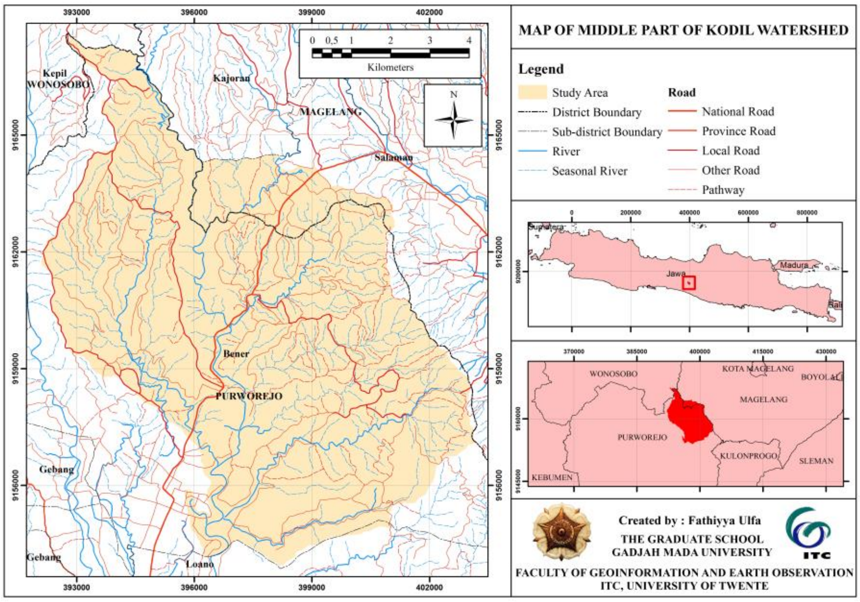

Figure 4.1. Map of middle part of Kodil Watershed

4.2 Altitude

The study area has elevation variety from 100 to 850 meters above sea level, which is distributed from low to high elevation from south to north. The south part of the study area until the middle part has variation in elevation between 100 to 400 meters above sea level, whereas the north part and several east part of the study area has more than 400m elevation. The north and east part are higher than other part because those sides is influenced by Sumbing and Menoreh mountain. Those varieties of elevations causes morphological different from plain to mountainous topography. The morphological different leads to landslide occurrence frequency. By the fact, several villages located in a mountainous area are prone to be affected by landslide occurrence, even could be inaccessible during landslide hazard.

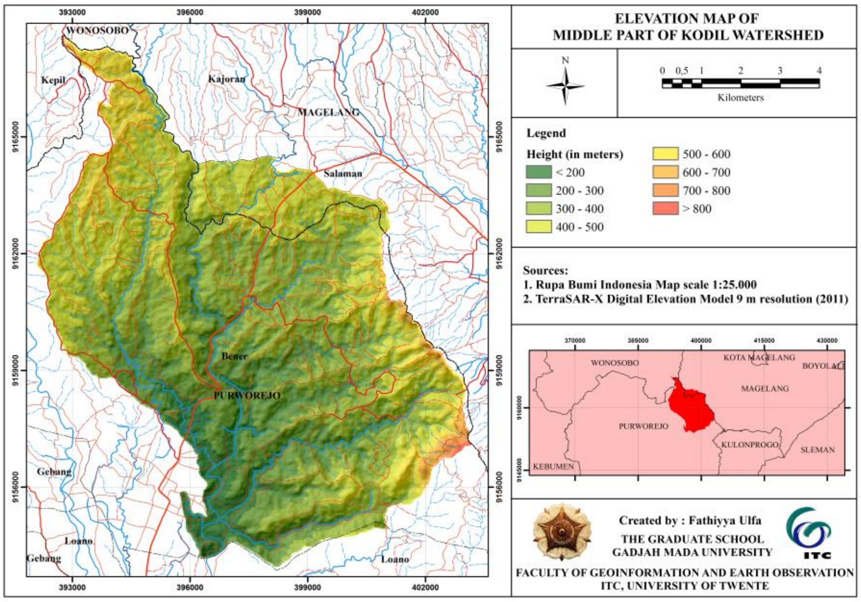

Figure 4.2. Elevation map of middle part of Kodil Watershed

4.3 Climatology

Beside the topography of the area, high rainfall intensity also causes the landslides occurrence. 7 rainfall stations, which are located not more than 5 km from the study area, was selected to represent the rainfall information. The rainfall stations are Banyuasin, Bener, Guntur, Kedungputri, Maron, Ngasinan, and Salaman. Based on those stations, the rainfall intensity was varied from 0 mm to 627 mm. According to the analysis of Figure 4.3, the peak of the rainfall season commonly occurred in December and January. Then commonly, after the peak season of rainfall, the landslides occurred, especially in the middle to the end of the rainy season when there was a continuous rainfall for more than 3 days.

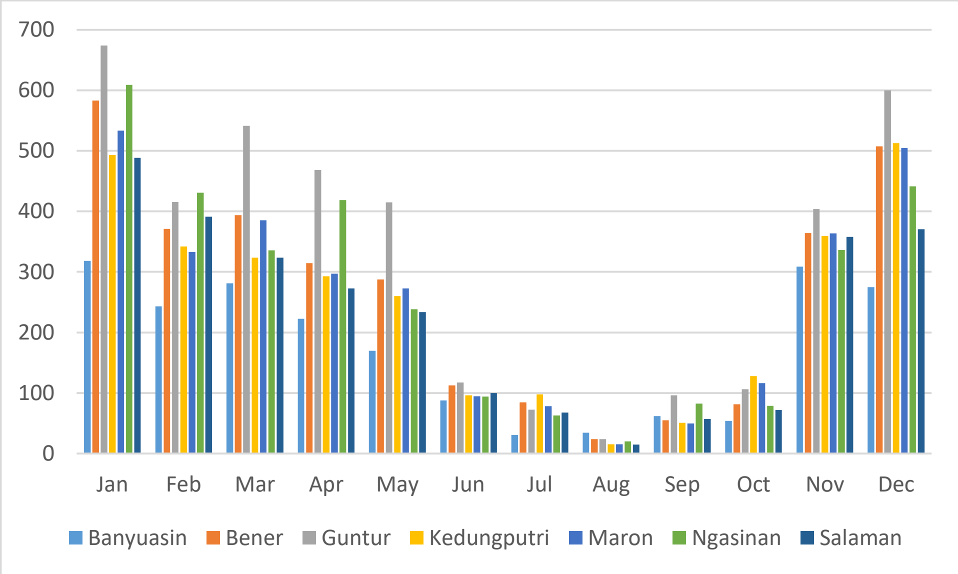

Figure 4.3. Average monthly rainfall 2009-2015

Figure 4.3 depicts that the rainy season was begun from November, while dry season was begun from June. All rainfall stations show similar trends between one station to another, except Guntur and Ngasinan stations which have much higher rainfall intensity than other. This difference happened because the stations are located in higher elevation than others (shown in figure 4.4). It is shown that the higher the station is located, the higher the rainfall intensity.

Based on Schmidt – Ferguson classification, the study area is categorized as a B climate type or wet climate. The class was generated from the ratio of dry and wet month. Generally, middle part of Kodil watershed has two dry months which has average monthly rainfall lower than 60 mm and 8 wet months which has average monthly rainfall higher than 100 mm.

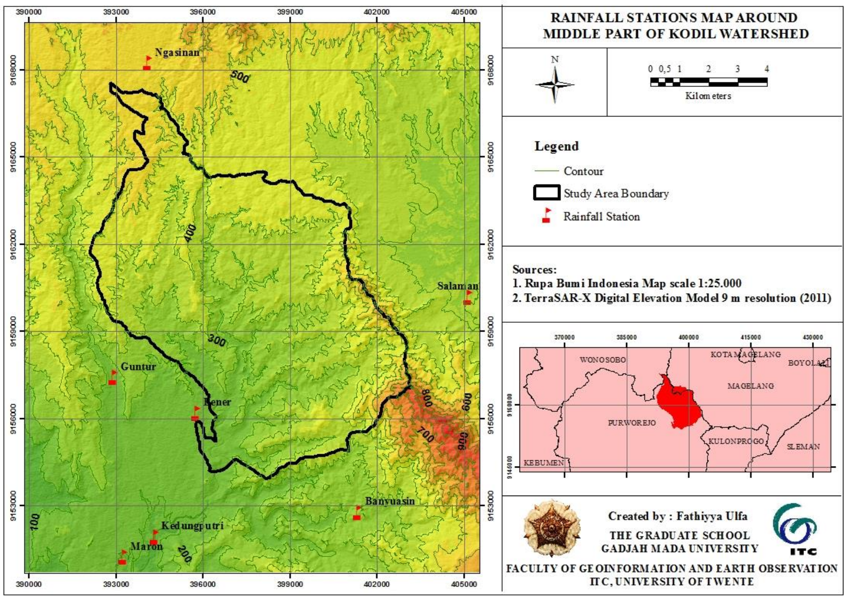

Figure 4.4. Rainfall stations map

4.4 Geology

The study area has four different geological formations including alluvium, old andesite formation, sentolo formation and andesite. From the four formations, old andesite formation is dominantly appears in the study area. Surficial deposits for old andesite formation are andesitic breccia, tuff, lapilli tuff, agglomerate and intercalations of andesitic lava flows. Then andesite surficial deposits consist of composition ranges from hypersthene andesite to hornblende-augite andesite and trachyandesite. On west side of study area, there are sentolo formation and alluvium. Sentolo formation dominantly consists of limestone and marl sandstone, while alluvium consists of gravel, sand, silt and clay along larger streams and coastal plain as surficial deposits.

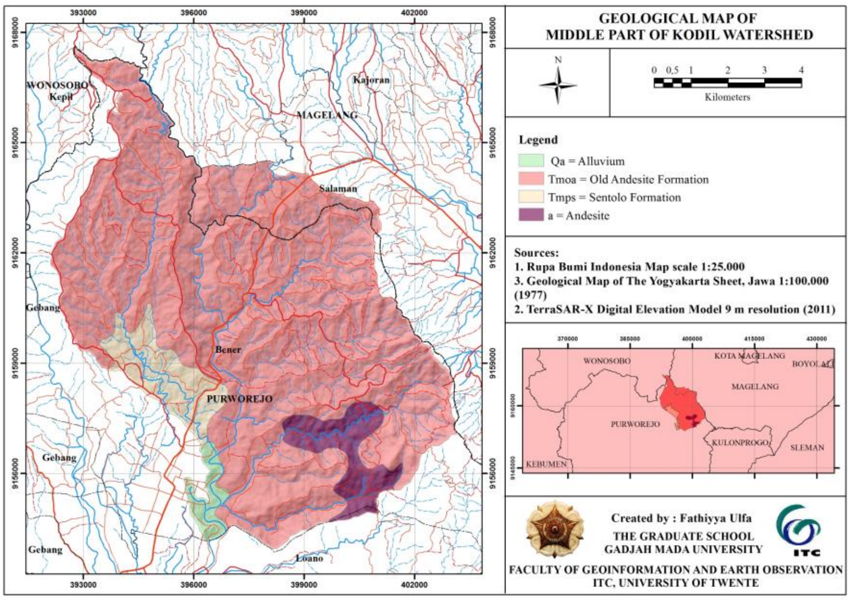

Figure 4.5. Geological map of middle part of Kodil Watershed

4.5 Land Use

Land use in the study area is dominated by plantation or commonly called a commercial forest. Almost in the whole part of the study area are dominated by the plantation land use. Aside from plantation, there is also a paddy field which commonly associated with rivers. It is different to dry farming land which is distributed irregularly in the study area. Other land use are savanna and shrub, they do not significantly exist in the study area since the area covered by those types of land use is not considerable. Aside from all land use, settlement is clearly seen in the study area. It is scattered clumps forming a hamlet and generally associated with roads, paddy field and dry farming land.

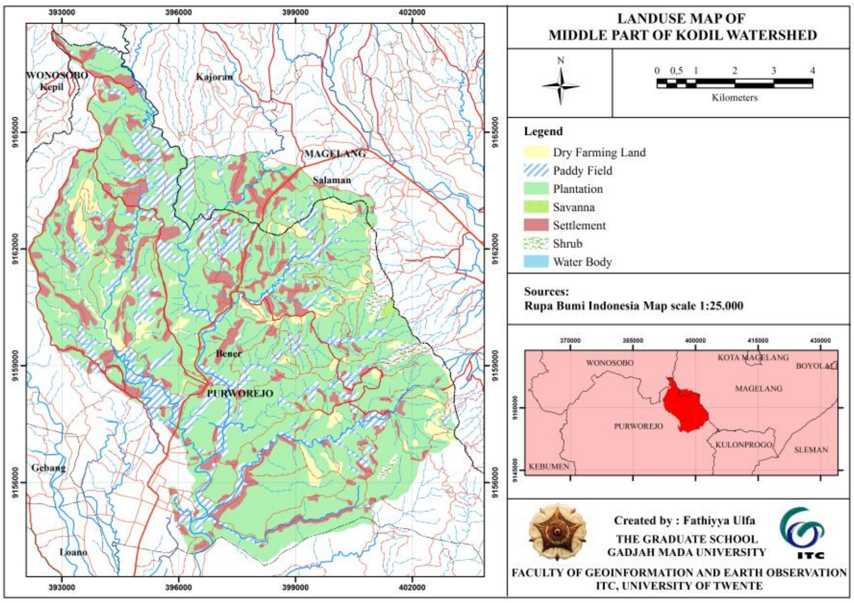

Figure 4.6. Land use map of middle part of Kodil Watershed

Aside from natural triggering factors, landslides in the Middle Part of Kodil watershed were also triggered by the poor land management, including undercutting slope by transportation activities (Rusdiyatmoko, 2013). As shown in figure 4.5, the main road passes through the study area. It is exacerbated by the main road which regularly used by logging truck, then cause vibration leading to landslides.

4.6 Landslides

Landslides in the study area frequently happen year by year. Recorded by Rusdiyatmoko (2013), from 2003 until 2013, 152 landslides occurred. After 2013, the data shown that still the landslides still frequently occurred with 50 events increased. Those landslides have the average length and width between 5 – 100 m, yet occasionally, the maximum length as well as width might reach 700 m distance.

Until 2013 there are 8 landslides with more than 100m long, then increase 4 events until 2016. Those huge dimensions indicate that there are possibility of huge landslide occurrence in the study area. The huge dimensions of landslides may lead material spreading caused by landslide run-out, then affects a destruction in the agricultural area, road network, and settlement.

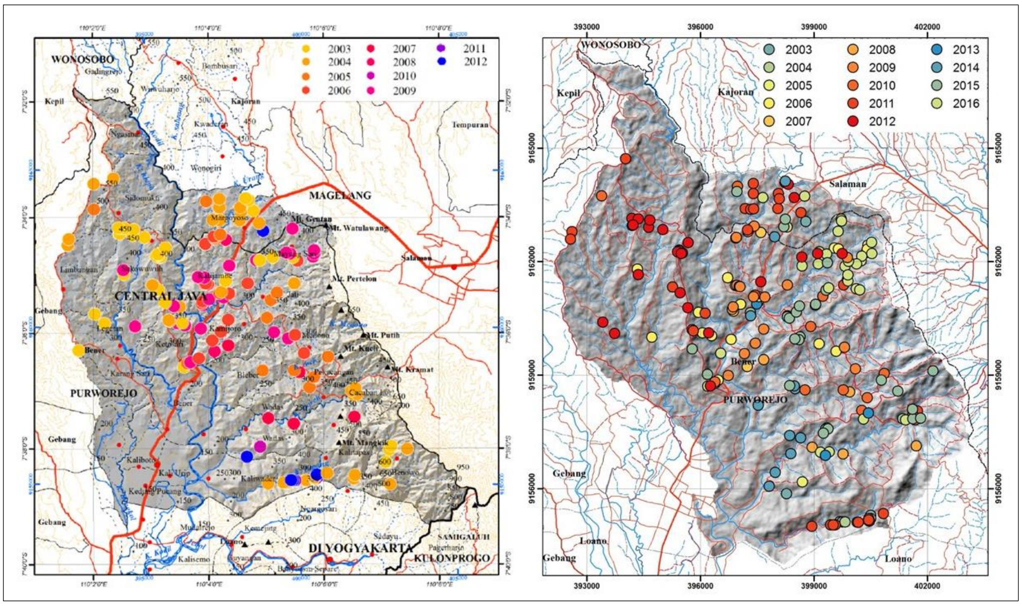

Figure 4.7. Landslide occurrence 2003-2013 (left), 2003-2016 (right)

The following table shows how the landslide frequency increase from previous inventory until recent inventory.

Table 4.2. Landslide length in middle part of Kodil Watershed

Landslide length (m)	**Frequency of events 2003-2013**	**Frequency of events 2003-2016**
Missing data	7	-
0-25	90	143
25-50	27	27
50-100	19	20
100-450	9	12
Total	152	202

CHAPTER 5. RESULT AND DISCUSSION

5.1 Landslides

5.1.1 Landslides Inventory

The landslide inventory was conducted by collecting data from previous research and governmental institution, namely BPBD (Badan Penggulangan Bencana Daerah). The inventory before 2013 was obtained from a previous study, while the inventory after 2013 was obtained from BPBD. The data consists of date, location, victim, losses and short description of landslide events. One of deficiency related to inventory data was not every point consist of coordinate information.

To reduce the deficiency of lack information about landslide coordinates, interviewing local authorities was applied. The respondents are head, secretary and staff of the villages. After the interview, respondents are being asked to mark the landslide location on the map. This method also used to determine landslide dimension including, the width and the length.

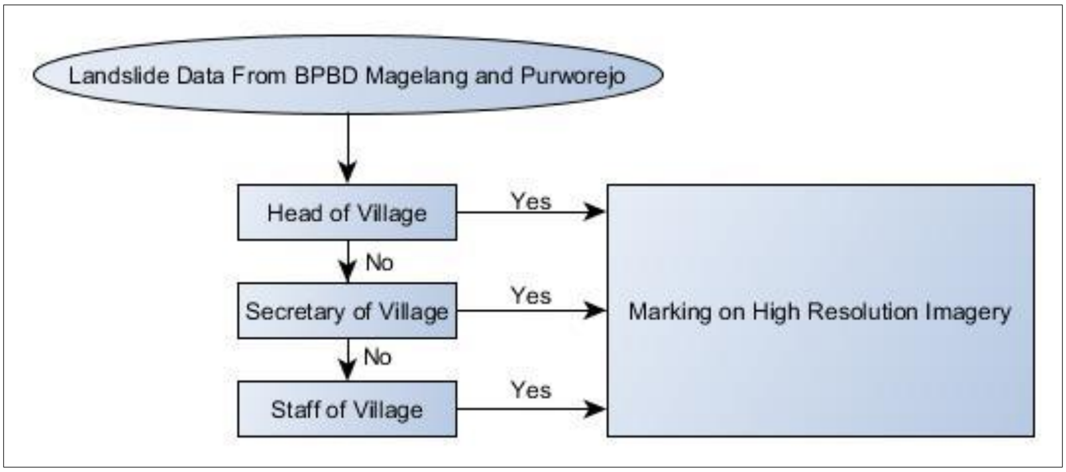

Figure 5.1. Hierarchy of landslide inventory

Table 5.1. Landslides inventory

No	Village	Year (20...)														Total
		03	04	05	06	07	08	09	10	11	12	13	14	15	16	
1	**Bener**															0
2	**Bleber**								1				3	1		5
3	**Cacaban Lor**									4		1		4	2	11
4	**Cacaban Kidul**															0
5	**Jati**				1				3	1			1	9	6	21
6	**Kalijambe**				6	1		13		2	1	1	2	1	1	28
7	**Kalitapas**						1			1						2
8	**Kaliwader**	3	2							11						16
9	**Kamijoro**					1	1	4								6
10	**Kedungloteng**															0
11	**Ketosari**				5				1	3	2	1		2	2	16
12	**Limbangan**															0
13	**Legetan**				1						2					3
14	**Margoyoso**	1							1	9	3		1	3	3	21
15	**Mayungsari**				6			1			3			1	13	24
16	**Medono**				1			2								3
17	**Ngasinan**															0
18	**Nglaris**								1	3						4
19	**Pekacangan**						1		4					3		8
20	**Sidomukti**															0
21	**Sokowuwuh**				1					1	16					18
22	**Wadas**	1		1			2					1	7	2	2	16
Total		5	2	1	21	2	5	20	11	35	27	4	14	26	29	202

As shown from table 5.1., total landslide occurred from 2003 are 202 events. The highest number of events occurred in Kalijambe village (28 cases), then the highest number of landslide event occurred in the year 2011 (42 cases).

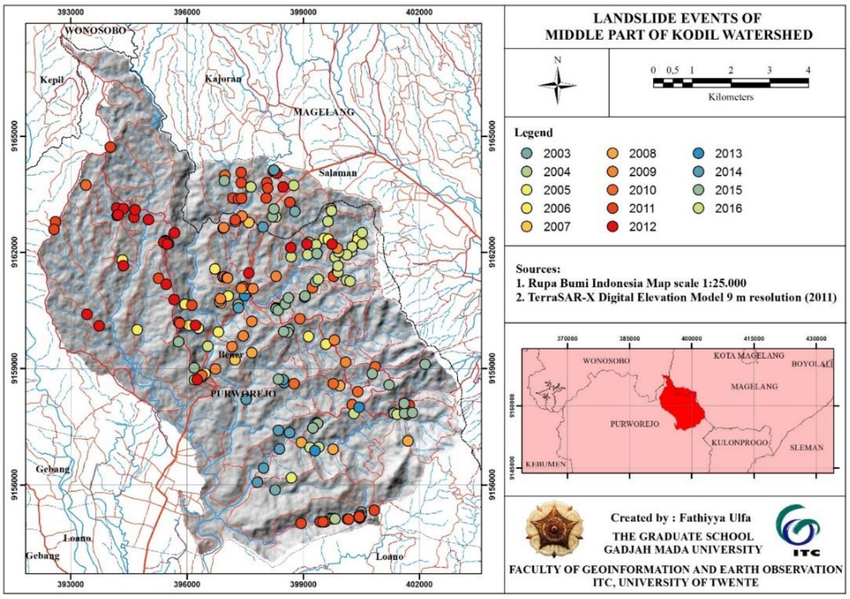

Figure 5.2. Landslide events of middle part of Kodil Watershed

5.1.2 Landslide Susceptibility Assessment

5.1.2.1 Landslides Density

Landslide density was used to determine landslide susceptibility based on the weight of evidence analysis. To build a landslide density map, it is necessary to determine landslide polygon in previous. The inventory data, which consist of landslide dimension, were used to determine the landslide polygon. Aside from the dimension, hill shade, which is extracted from the 9 meter DEM (Digital Elevation Model) and high resolution imagery was used to interpret the landslide polygon. From the data collected from 2003 to 2016, landslides occurred in 21,52 ha from 7951,22 total area, which means, the landslide density is around 0,0027 or in other words 0,2 % of the total area was exposed by landslides.

Figure 5.3. Landslides in the study area

5.1.2.2 Rainfall

Rainfall data, which were used for landslide susceptibility analysis, were taken from 7 rainfall stations, including Banyuasin, Bener, Guntur, Salaman, Ngasinan, Maron, Kepil, and Kedungputri. In general, landslide cases are not only influenced by rainfall intensity, but also rainfall duration (Kritikos & Davies, 2014). Therefore, maximum three days rainfall is more appropriate to be used for analysis than only using a traditional daily rainfall or annual rainfall. In Indonesia, many rainfall stations not have adequate data for daily rainfall, some are clearly available, while some data were broken due to equipment error as well as human error. In this research the data used are the data from 2009 to 2015 since in that period of time, the data of daily rainfall are clearly available.

Table 5.2. Maximum 3 days rainfall

Years	**Rainfall Stations**						
	Banyuasin	Bener	Guntur	Salaman	Ngasinan	Maron	Kedungputri
2009	197	201	270	231	195	198	166
2010	130	244	305	168	203	224	207
2011	79	176	230	161	253	199	231
2012	82	264	235	217	200	192	224
2013	94	182	226	159	217	207	315
2014	81	229	194	155	199	182	199
2015	59	156	263	216	185	173	150
Rmax	197	264	305	231	253	224	315

The highest 3 days cumulative rainfall was recorded in Kedungputri station with a value of 315 mm. On the other hands, the lowest value was recorded in Banyuasin station with a value of 197 mm. To get spatial distribution of maximum 3 days cumulative rainfall, isohyet method was applied. Each station has its own value of maximum 3 days cumulative rainfall, then the value was interpolated to the other nearest station to get the spatial distribution of the value.

From the interpolated result, 3 days cumulative rainfall was classified into 2 classes, including the class of lower than 250 and higher than 250 mm. Generally, the 3 days cumulative rainfall was increased from east to west part of the study area. It is linear to the elevation of the area which also increased from the east to the west. Based on the area, the value of 3 days cumulative rainfall is dominantly higher than

250 mm, only one-fourth of the area which has lower than 250 mm 3 days cumulative rainfall.

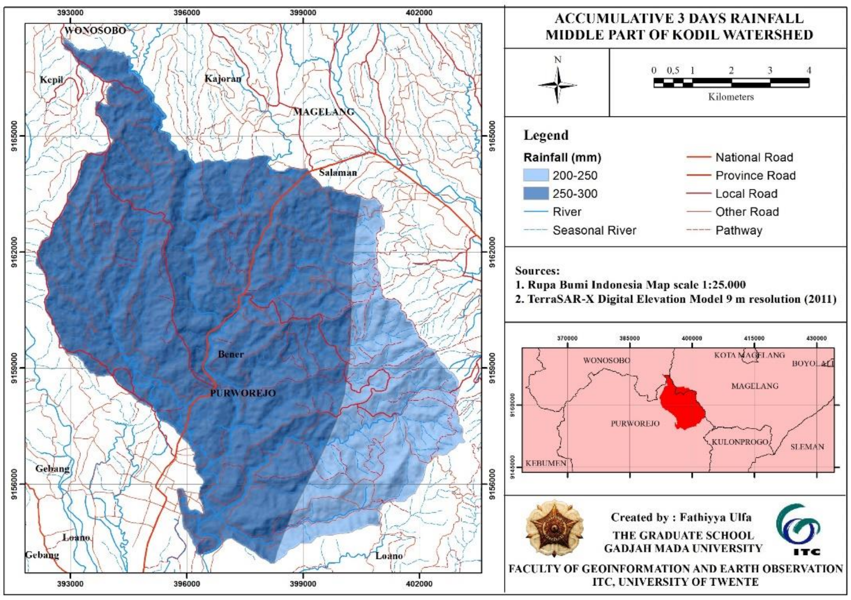

Figure 5.4. Three days cumulative rainfall of middle part of Kodil Watershed

Based on rainfall classification and weight of evidence analysis, most landslides occurred in the area with 3 days more than 250 mm with 19,14 ha area was exposed by landslides, or in other words, the class received the highest weight and expected to be dominant rainfall class causing landslide occurrence. On the other hands, the area with 3 days cumulative rainfall less than 250 mm only had 2,38 ha extent area exposed by landslide. The weight of both classes showed that the class of more than 250 mm rainfall perceived higher value than the class of less than 250 mm rainfall. It showed that the area with 3 days cumulative rainfall more than 250 mm is more susceptible to landslide than the area with less than 250 mm 3 days cumulative rainfall.

Table 5.3. The weight calculated for rainfall parameter

Classes	Area (ha)	Landslide Area (ha)	Weight
200 - 250	1747,9	2,38	-1,3802
250 – 300	6203,3	19,14	0,263

5.1.2.3 Geology

Parent rock of the study area is dominantly breccia, which easily to weather and producing thick silt to clay soil. Generally, breccia in a tropical climate will be weathered into sandy-clay, clayey-sand, and sand-clay. Those types of soil have a low shear strength which consequently is most sensitive to fail (Karnawati, 1998). Breccia is dominated in Tmoa (Old andesite of Bemmelen Formation) geology class, which is the dominant class in the study area. Besides, there are also other classes which not too dominant, namely andesite (a), alluvium (Qa) and sentolo formation (Tmps) dominated with limestone and sandstone.

Based on the evidence of recorded landslide, Tmoa received the widest area which is exposed by landslide. It is proved by the weight of Tmoa class which is the highest weight among other classifications. Sentolo formation and alluvium class are not significantly caused landslides since the area exposed by landslide are almost zero and the weights are very low.

Table 5.4. The weight calculated for geology parameter

Classes	Area (ha)	Landslide Area (ha)	Weight
Tmoa	6860,56	21,24	0,263
Tmps	496,62	0,01	-7,103
Qa	159,72	0	-10,626
a	434,72	0,27	-3,755

The old andesite in the study area was formed between Oligocene to Miocene. In the study area, the old andesite formed as a result of volcanic activities of Menoreh Mountain. Due to the high activity of some mountains surrounding the Menoreh Mountain, it was elevated and lift up its mantle consisting andesitic breccia. This activity made the intrusion of dacitic rock in some area and as time goes by the the dacite rocks were shifted to the lower part, so that the old andesite formation with breccia dominated the surface area. (Bemmelen, 1949)

5.1.2.4 Land Use

The land use in the study area is dominated by plantation or commonly called a commercial forest. Almost in the whole part of the study area are dominated by the plantation which is many kinds of woody trees are planted such as durian, jackfruit, coconut, hardwood trees and albizia. Aside from plantation, there is also dry farming land which is dominated by corn and nuts cultivated. Generally in the study area, settlement is scattered clumps forming a hamlet. Ordinarily, in association with the settlements, paddy fields are cultivated.

Figure 5.5. Land use in the study area

Based on land use classification from Badan Informasi Geospatial (BIG), where the land use data sourced, the land use in the study area is classified into 8 classes, including dry farming land, lake, paddy field, plantation, river, savanna, settlement and shrub. Among those classifications, the plantation is the dominant land use in the study area with 5206,02 ha total area, while the most narrow land use classification is the lake with only 1,33 ha total area. Due to the wide area of plantations, many landslides occurred in that land use class. Around 12,09 ha area exposed by landslide were located in the plantation. The second place where received the landslide exposure was paddy field with the 6,22 ha total area. Aside from that fact, the weight causing landslide from paddy field is higher than plantation which consist of the widest exposed landslide area. This fact was led by the density of the landslides in paddy field is higher than plantation. It is proved by wide landslide area in paddy filed which is 6,22 ha from 1053,9 ha total paddy field area, while in plantation area which is 5 times wider than paddy field only exposed 2 times higher than it from paddy field specifically 12,09 ha from 5206,02 ha total area. Based on the weight calculated, there are 4 land use classes which not favorable to landslide occurrence namely lake, river, savanna and shrub.

Table 5.5. The weight calculated for land use parameter

Classes	**Area (ha)**	**Landslide Area (ha)**	**Weight**
Dry farming land	424,33	0,92	-0,13
Lake	1,33	0	-3,477
Paddy Field	1053,9	6,22	1,091
Plantation	5206,02	12,09	-0,285
River	97,96	0	-7,79
Savanna	17,07	0,001	-3,468
Settlement	1069,43	2,29	-0,157
Shrub	81,15	0	-7,6

In the study area, the land use change was extensively occurred. Most of the paddy field was built due to land use change from the natural vegetation. It happens because of the high demand of economic needs, so the exploitation of land resource occurred. It is not often that the paddy field was cultivated on the steep slope which lead to the instability of the slope. Besides, the paddy field cultivation leads the high intensity of land treatment since the paddy is plant 2 times a year, so that the instability of the slope is increased.

The existence of this type of paddy field also leads the instability of plantation area which was associated it. The plantation area which located in the upper part of the paddy field will face the effect of the instability of the paddy field area. Therefore, it is also often the landslides occurred in the plantation. It can be concluded that the paddy field area, especially the one which is cultivated due to land use change from the natural vegetation, is prone to landslides. Then, the plantation which is associated to the paddy field is also prone to landslides.

5.1.2.5 Slope and Landform Combination

In this research, slope and landform where classified into one factor map due to their influence one to another. Every landform unit is characterized by predominant process on it, which influence the stability of the area (Swanson et al., 1988). Those predominant processes influence the sensitivity of an area to landslide in a certain slope. For instance denudational landform is dominated by erosional process which more sensitive to the landslide although on the gentle slope. This condition might be different through other landform unit. It can be concluded that the same slope classification may have different influence to landslide occurrence due to the predominant process difference of a landform. A certain landform may sensitive to landslide occurrence in the slight slope, otherwise a certain landform may not sensitive to landslide occurrence even in the steep slope.

The slope data were differentiate into 5 categories which have different area extent as depicted in table 5.6 and figure 5.6.

Table 5.6. Slope area

Class	Slope (%)	Area	
		Ha	**%**
I	0 - 15	1413,857	17,78
II	15 - 25	2049,117	25,77
III	25 - 45	3444,98	43,33
IV	45 - 65	920,568	11,57
V	> 65	121,411	1,53

Slope data was extracted from Terrasar DEM which has 9 m pixel length. Generally, slope the study area are categorized as moderate which has a value of 25 – 45 %. Among all the area, 43,33% area is included in this class. The highest degree of slope area is distributed in the south east side of the study area. Commonly, an area which is categorized as class I is used for the paddy field area and settlement. In contrast, area which is categorized as class V is generally used for plantation such as durian, jackfruit, coconut, hardwood trees and albizia.

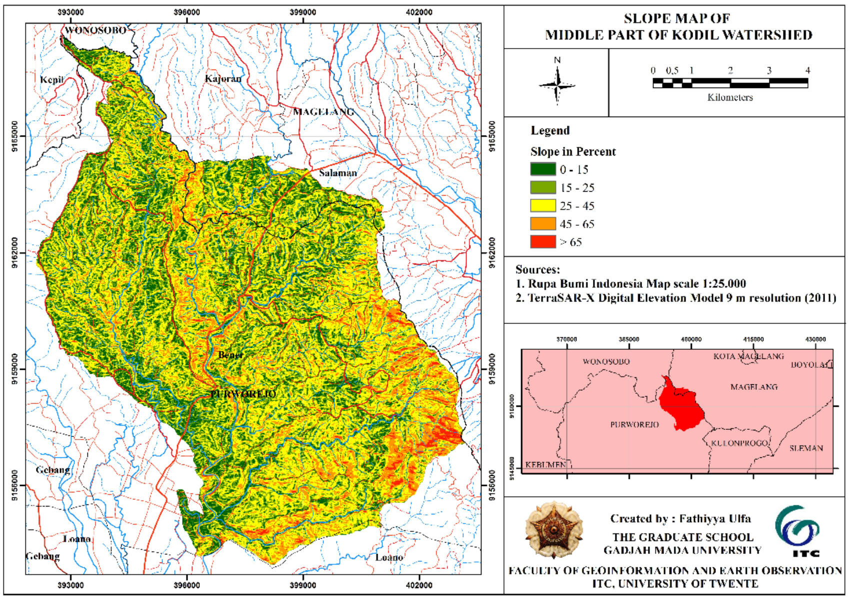

Figure 5.6. Slope map of middle part of Kodil Watershed

Subsequently, landform map was interpreted using 3 main data, including Pleiades imagery, geology and hill shade which is extracted from terrasar imagery. From the interpretation, landform was classified into 3 classes, namely structural, volcanic and denudational class. The structural class, which is influenced by menorah mountainous area, is dominated in the eastern part of the study area, while volcanic class, which is influenced by Sumbing Mountain, is dominated in the west part of the study area. In addition, in the middle part of the study area, denudational process is significantly formed.

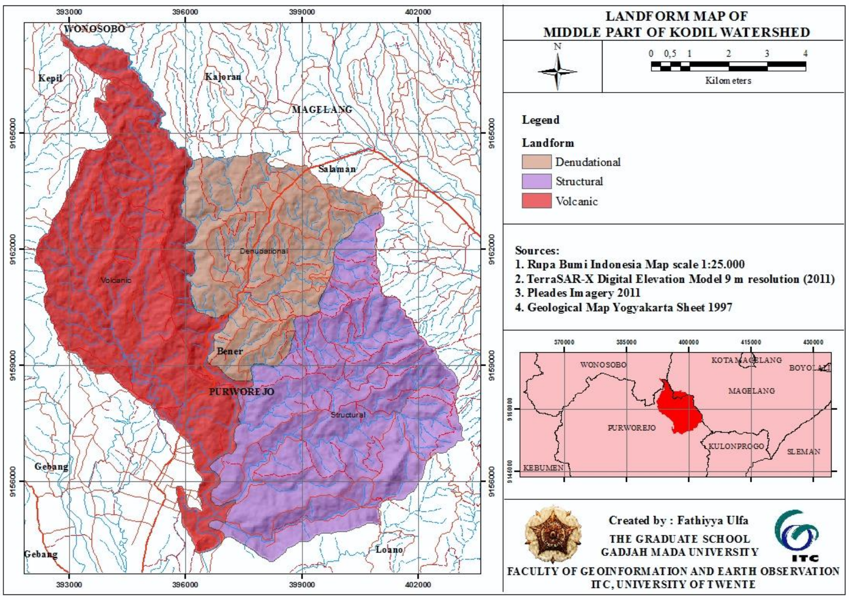

Figure 5.7. Landform map of study area

Here is the area distribution of the landform;

Table 5.7. Landform area

Class Code	Landform	Area	
		Ha	%
D	Denudational	1812,32	22,79
SM	Structural, Menoreh mountainious influence	3088,45	38,84
VS	Volcanic, Sumbing mountain influence	3050,42	38,36

After the class of the slope and landform were identified, both maps are overlaid to get the combination of both of them. Then, the combination data were used as one of factor map in weight of evidence analysis. In total, the classification consists of 15 classes, including 5 slope classes in each landform class.

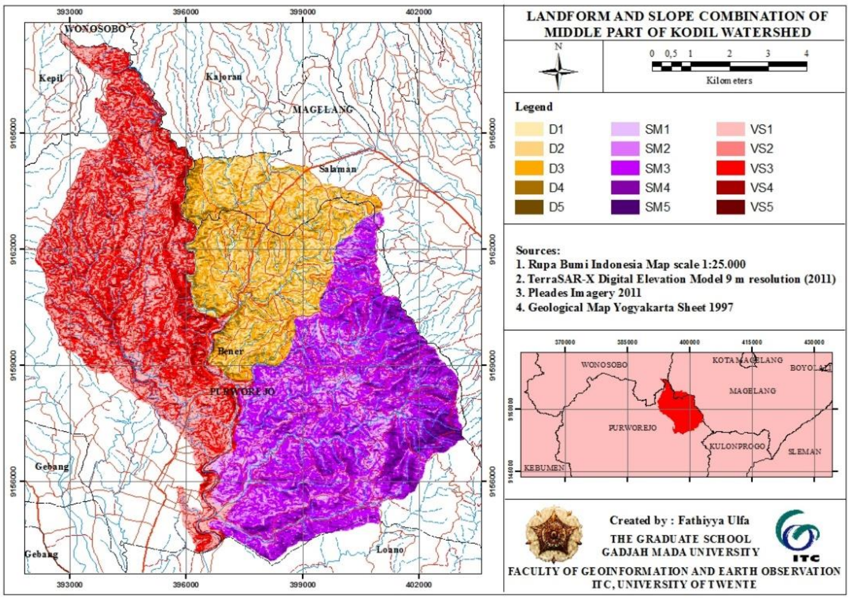

Figure 5.8. Landform and slope combination

Generally, the landslide occurrence was distributed equally in all classes. It is showed the following table under the landslide area column which have a value around 0 to 3 ha. From the following table, if it is only seen from the extent of landslide exposure area, the landslides occurred mostly in slope classes around 25-45%. It is shown from the landslide area which are 2,66 ha in structural, 3,04 ha in volcanic and 3,59 ha in denudational landform.

Aside from that, the weight for each class not only depends on the total area exposed by a landslide, but also depend on the total area of each class. In other words, it depends on the density of landslides in each class. The highest weights are received by denudational landform with different slope classes, whereas other landform such as volcanic and structural are not showing the significant difference. It is proved that denudational landform is more sensitive to landslide than structural and volcanic. It is because the denudational landform are prone to be eroded. The highest weight is received by denudational landform with 25 to 45% class of the slope, while the lowest weight is received by volcanic landform with more than 65% slope.

Table 5.8. The weight calculated for slope and landform combination

Classes	**Slope (%)**	**Landform**	**Area (ha)**	**Landslide Area (ha)**	**Weight**
SM1	0-15	Structural	332,23	1,05	0,167
VS1	0-15	Volcanic	699,15	1,61	-0,173
D1	0-15	Denudational	358,52	1,47	0,444
SM2	15-25	Structural	643,4	2,22	0,268
VS2	15-25	Volcanic	886,17	2,2	-0,095
D2	15-25	Denudational	529,75	1,85	0,279
SM3	25-45	Structural	1486,34	2,66	-0,49
VS3	25-45	Volcanic	1196,85	3,04	-0,075
D3	25-45	Denudational	765,67	3,59	0,632
SM4	45-65	Structural	532,61	0,89	-0,505
VS4	45-65	Volcanic	240,27	0,29	-0,821
D4	45-65	Denudational	147,13	0,6	0,418
SM5	>65	Structural	93,59	0,03	-2,293
VS5	>65	Volcanic	21,25	0	-6,36
D5	>65	Denudational	12,56	0,006	-1,705

5.1.2.6 Level of Landslide Susceptibility

Landslide susceptibility in the study area was constructed from 4 basic landslide susceptibility parameters including rainfall, geology, land use and the combination of slope and landform. First of all, the landslide occurrence map was constructed to know landslide distribution and its density. The landslide occurrence map later was overlaid with each factor map to get the positive and negative weights of each class using weights of evidence equation, which was described in methodology chapter. In general, the presence of one class in a certain parameter implies the absence of the other class. So that to get the cell weight in each parameter map, the positive weight of a certain class in a cell was added by the negative weight of the other classes in the same map. On the other hands, it was also reduced by the negative weight of the class itself.

The weight of each class from rainfall, geology, land use and slope-landform combination was consecutively shown in table 5.3, 5.4, 5.5, and 5.8. Based on the weight of evidence analysis, highest weight of each factor maps was received by 250-300 mm rainfall, old andesite formation (Tmoa), paddy field and denudational landform with 25-45% slope. It was shown from the highest value of the weight that have been calculated in previous.

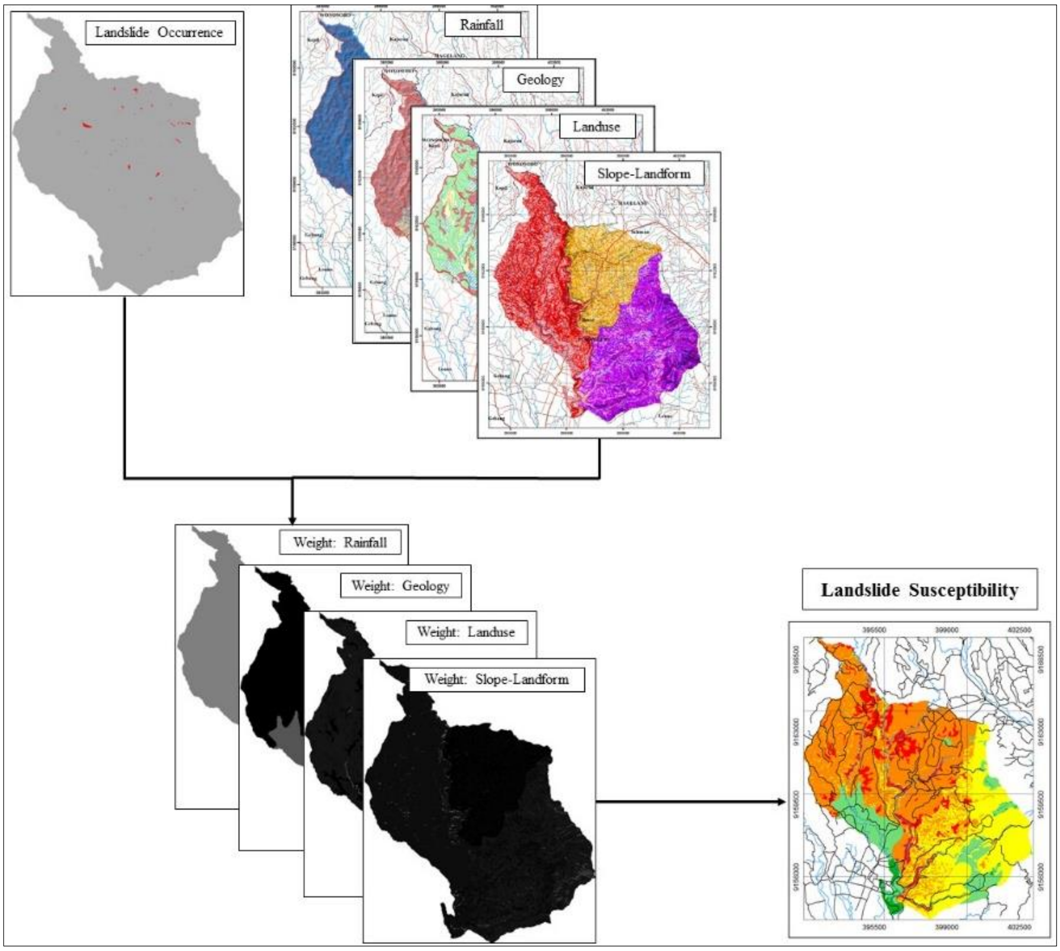

Figure 5.9. Simplified flowchart of weight of evidence analysis

To get the final weight in landslide susceptibility identification, all weights gained from individual parameter maps were summed up to get the final weights of each cells in the study area. The summed up weight, which is varied from -24,512 to 2,249, was classified as the following table to get susceptibility classifications. The weight of cell which has a value lower than -10 was classified as very low susceptibility since the value were resulted from the class which has no landslide. In the other hands, all the positive weights were categorized as high and very high susceptibility.

Table 5.9. Classes of landslide susceptibility

Class	**Lower Bound**	**Upper Bound**
Very low	-24,147	-10
Low	-10	-5
Moderate	-5	0
High	0	1,125
Very high	1,125	2,616

According to final susceptibility analysis, most of the area was classified as high susceptible to landslide with total area around 3836,76 ha. While the smallest area was classified as very low with only 134,19 ha total area. Then very high, moderate, and low classification were consecutively has value 675,4 ha, 2308,51 ha, and 990,63 ha.

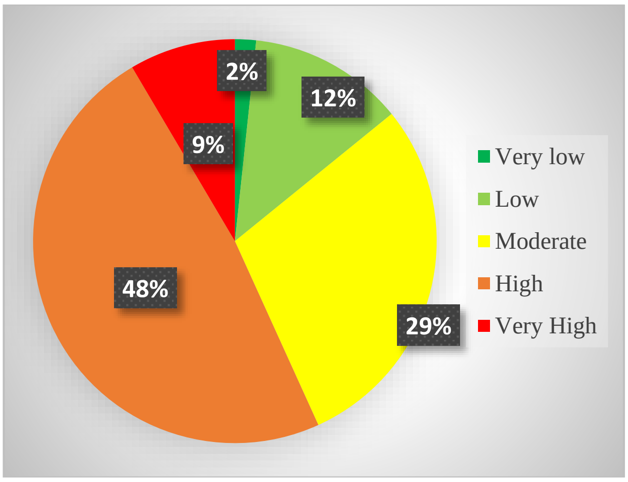

Figure 5.10. Percentage of landslide susceptibility level

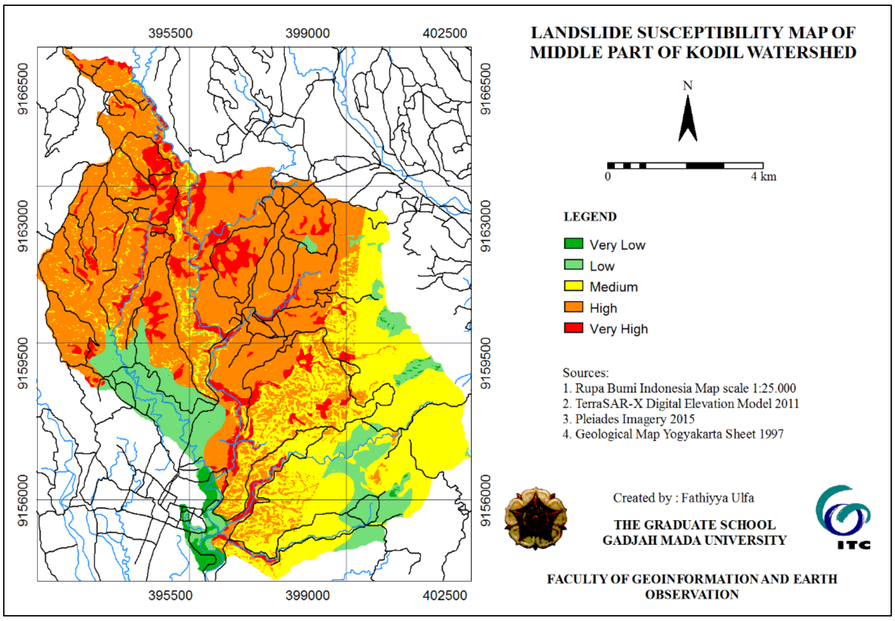

Figure 5.11. Landslide susceptibility map

The level of landslide susceptibility showed the correlation compared to recorded landslide events,. It was proved by the amount of events which occurred in the very high and high class of susceptibility. From recorded data, 8 events occurred in very high class, 125 events in high class, 55 events in medium class, 14 events in low class, and no landslides occurred in very low class.

5.2 Debris Flow

In this research, 3 debris flow events were modelled to identify specific parameters causing their occurrence using back analysis method. Generally, the events chosen for debris flow modelling are the landslide which has lengths more than 100 meters. From the inventory data, there are 11 events from 2003 until 2016 that meet those criteria and 3 recently events are chosen to be modelled. The selected event was chosen because no significant interference occurred to them, so the extent area was still naturally built. From the following table, the last three events were chosen which located in Jati, Margoyoso and Mayungsari village. Furthermore, debris flow event in Margoyoso will be referred as first debris flow, Mayungsari as second debris flow and Jati as third debris flow.

Table 5.10. Debris flow inventory

No	Date	Village	X	Y	Length	Width
1	January 2004	Kaliwader	399817	9155118	150	20
2	January 2005	Wadas	398689	9156177	200	11
3	January 2006	Jati	399134	9159827	250	82
4	February 2009	Kalijambe	397417	9162941	120	30
5	February 2009	Kamijoro	397666	9160222	200	86
6	20 December 2011	Margoyoso	398055	9163805	182	121
7	1 January 2012	Sokowuwuh	395521	9162229	450	130
8	1 January 2012	Sokowuwuh	394626	9162913	130	89
9	9 November 2016	Jati	400117	9161284	320	30
10	9 November 2016	Margoyoso	398286	9162916	130	30
11	9 November 2016	Mayungsari	400531	9162216	700	40

5.2.1 Debris Flow Modelling

5.2.1.1 First Debris Flow

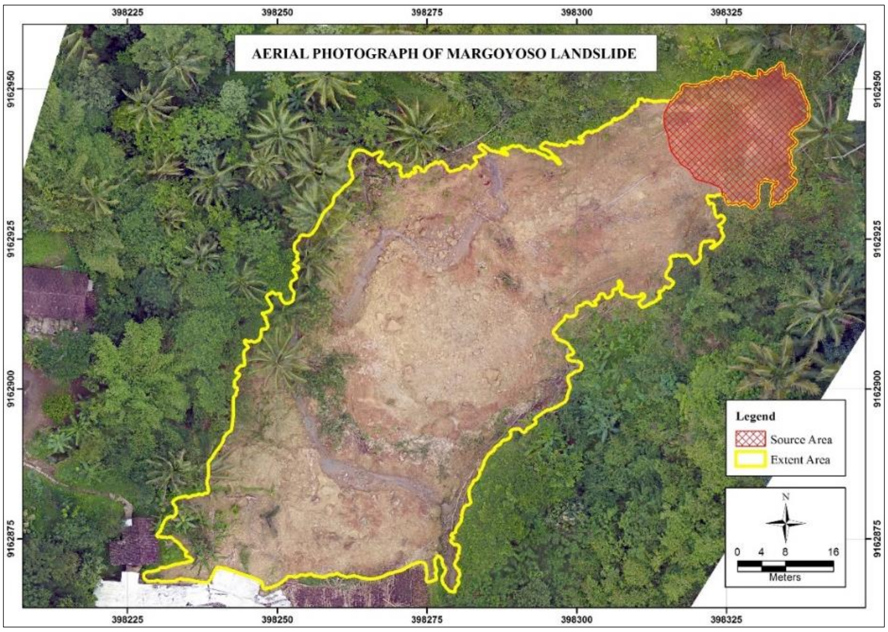

Figure 5.12. Aerial photo of first debris flow

The first selected debris flow event occurred on 9 November 2016 in Margoyoso Village around 4 PM. This debris flow event was triggered by extensive rainfall from several days before and was worsened by continuous rainfall from 12 PM on the occurrence day. The source area of the debris flow was a cliff which was more or less have a height of 40 m. The flow of material caused material spreading to more or less 4296 m^2 area with 130 m runout distance.

Modelling was calculated using release information inputs which were obtained from the fieldwork. The extent of release area was obtained by digitizing polygon based on imagery that was extracted from aerial photographs. It is located at 477,42 m altitude and 22,15° angle which is automatically calculated by the software after digitizing process. From the imagery interpretation, the value for release height and the extent are 11 m and 59,4063 m^2, respectively, which resulted 805,869 m^3 release volume.

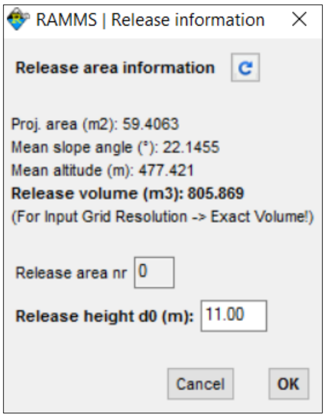

Figure 5.13. Release information of first debris flow

Beside release information input, there are also other input parameters which were obtained from literature and laboratory analysis including simulation and friction parameters. The simulation parameters such as, grid resolution, end time and dump step were selected as needed, commonly the default value was suggested. For other parameters such as, the soil density (ρ), earth pressure coefficient (λ), viscous turbulent friction (ξ), dry coulomb friction (μ) and the cohesion (c) were obtained from soil classification that is obtained from soil laboratory analysis, then further using literature to determine the exact value of each parameter. The value are 1850 , 0,38 , 200 , 0,51 and 0, respectively.

Table 5.11. Parameters value of first debris flow

Parameters		Value
Simulation parameters	Grid Resolution (m)	1,5
	End time (s)	1000
	Dump step (s)	5
	Density (kg/m^3)	1850
	Earth pressure coefficient	0,38
Friction parameters	Viscous-turbulent friction	200
	Dry-coulomb friction	0,51
	Cohesion	0

The combination of several input parameters resulted output value as summarized in the following table;

Table 5.12. Output of first debris flow

Output	Value
Simulation duration (s)	240
Max velocity (m/s)	18,01
Max flow height (m)	16,01

The simulation of debris flow was formed in 240 seconds duration with maximum velocity occurred in the beginning part of simulation where the release area started to collapse. The high velocity occurred in the first 15 seconds of the simulation, then continuously slightly moving until reaching low flux condition in the last second. The maximum velocity around the release area showed higher value compared to the velocity on the following part.

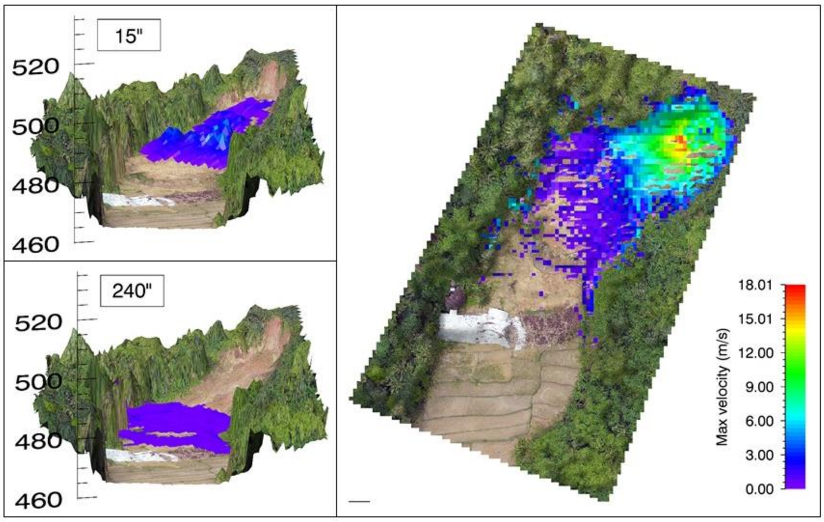

Figure 5.14. First debris flow simulation (left) and the maximum velocity (right)

The debris flow started with average height 11 meters at the release area. Subsequently, it spread to the area surrounding the source area with the average height between 5 to 2 m, then finally the material spread to the lower part with the height around 1 to 0 m until the flow stop. Generally, the high flow height only happen in the source area, while evenly the flow height is lower than 4 meters.

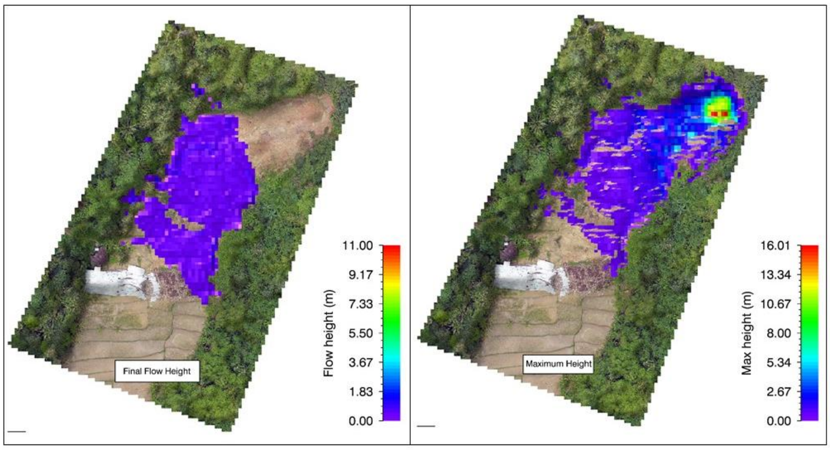

Figure 5.15. Final flow height (left) and maximum flow height (right) of first debris flow

5.2.1.2 Second Debris Flow

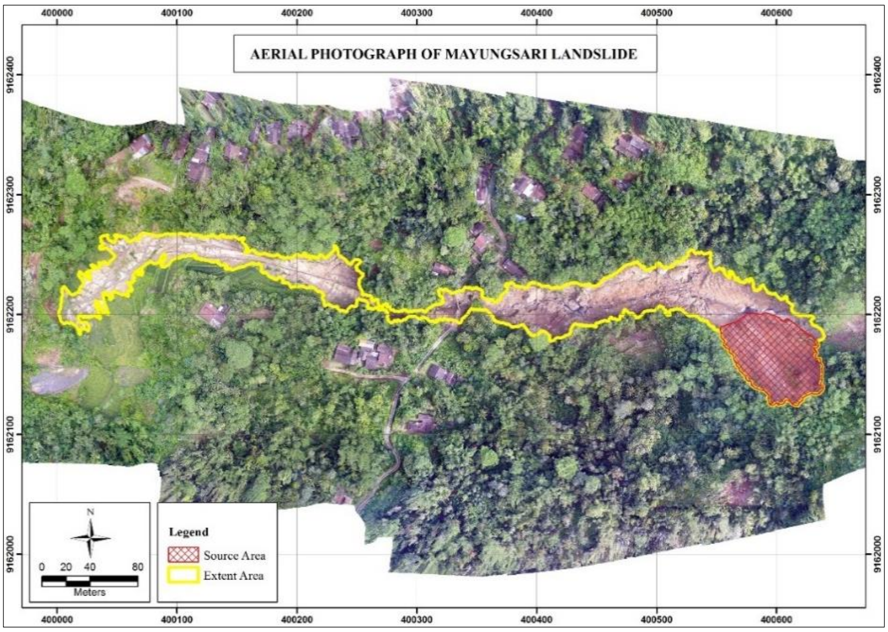

Figure 5.16. Aerial photo of second debris flow

The second debris flow event is located in Mayungsari village which also occurred on 9 November 2016. This debris flow event is the widest event among the other two events which has 2,2 ha area extent. It is located 2 km away from the first debris flow, so that the triggering factors causing the occurrence are almost the same. It was triggered by the extensive rainfall from several days before debris flow occurrence, then worsened by the high intensity of rainfall from 12 PM in the current day. The high loss, such as agriculture and infrastructure losses, are received due to this debris flow occurrence. One bridge which is the main road connecting one hamlet to another, is reported interrupted due to this occurrence.

From imagery interpretation and fieldwork, the release area information was obtained, then was digitized on the model interface which was extracted from aerial photographs. The release height was 16 m while the extent area was 787,063 m^2. The extent area and the height determined the material released which has the volume about 17182,6 m^3. This source area was laid in 454,48 m altitude and with 34,34° slope.

Figure 5.17. Release information of second debris flow

From laboratory test of the soil, based on USCS, the soil in second debris flow is classified as well graded sand or commonly known as SW which has friction angle value about 33°. From the literature, the well graded sand has the soil density (ρ) around 1850 kg/m^3, viscous turbulent friction (ξ) around 100 to 200 and zero cohesion. The value of viscous turbulent friction (ξ) between 100 and 200 represents the granular material. The higher the value, the smaller the particle. Value of 200 was chosen because the soil is not too gravelly. Furthermore, earth pressure coefficient (λ) and dry coulomb friction (μ) has value about 0,29 and 0,65, which calculated by the equation which was described in the methodology chapter.

Table 5.13. Parameters value of second debris flow

	Parameters	**Value**
Simulation parameters	Grid Resolution (m)	1,5
	End time (s)	4500
	Dump step (s)	5
	Density (kg/m^3)	1850
	Earth pressure coefficient	0,29
Friction parameters	Viscous-turbulent friction	200
	Dry-coulomb friction	0,65
	Cohesion	0

Based on aerial photography captured in the fieldwork, the area for the second debris flow is the widest area compared to the other two debris flow. It also proved by the simulation duration of the debris flow, which finished in 4010 seconds or 1 hour and 6 minutes. The maximum velocity almost reached 150 m/s, which also occurred in the beginning of the debris flow or near to the area where source volume was collapsed. Besides, the maximum flow height was recorded higher than the release height due to the obstacle faced by the material during the flow.

Table 5.14. Output of second debris flow

Output	Value
Simulation duration (s)	4010
Max velocity (m/s)	149,95
Max flow height (m)	58,6707

From the following figure, it is shown that the flow had higher velocity at the beginning of the simulation then gradually flow until reaching the maximum run-out area. In the first 500 seconds the debris flow reached almost two-third runout distance, but then the debris flow finished in in almost 1 hour later. It is proved by the maximum velocity chart in the figure which showed the high velocity in the first two-third runout distance then significantly decreased afterward. It happened due to the slit in a certain part was too small, so that the material was not flow immediately to the lower zone. The existence of hard rock around the slit caused the obstacle of the flow. A small bridge located in the slit, which is also a local street in that area, was destroyed due to the accumulative material during the flow.

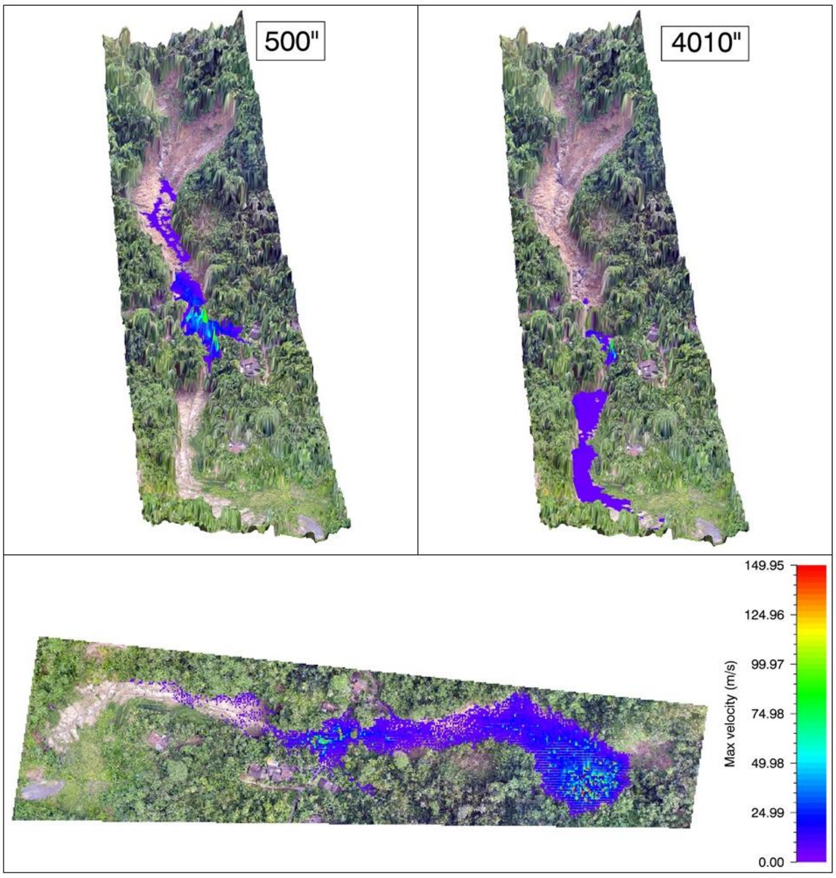

Figure 5.18. Second debris flow simulation (above) and the maximum velocity (below)

As same as the velocity, the maximum flow height of the second debris flow was also significantly different between the first two-third run-out distance and the rest. The first two-third distance has maximum height more than 4 meters, while the rest only has maximum height lower than 2 meters height. Generally, the significant flow height showed in the release area which has the height around 16 meters. At the end of the simulation, the overall release volume, which is 17182,6 m^3, was deposited in the half lower part of the extent area. From the simulation it was calculated that there is no material deposited from the release area until the middle part of the runout area. Those conditions were derived from the topography and material released characteristic which are represented in the model input.

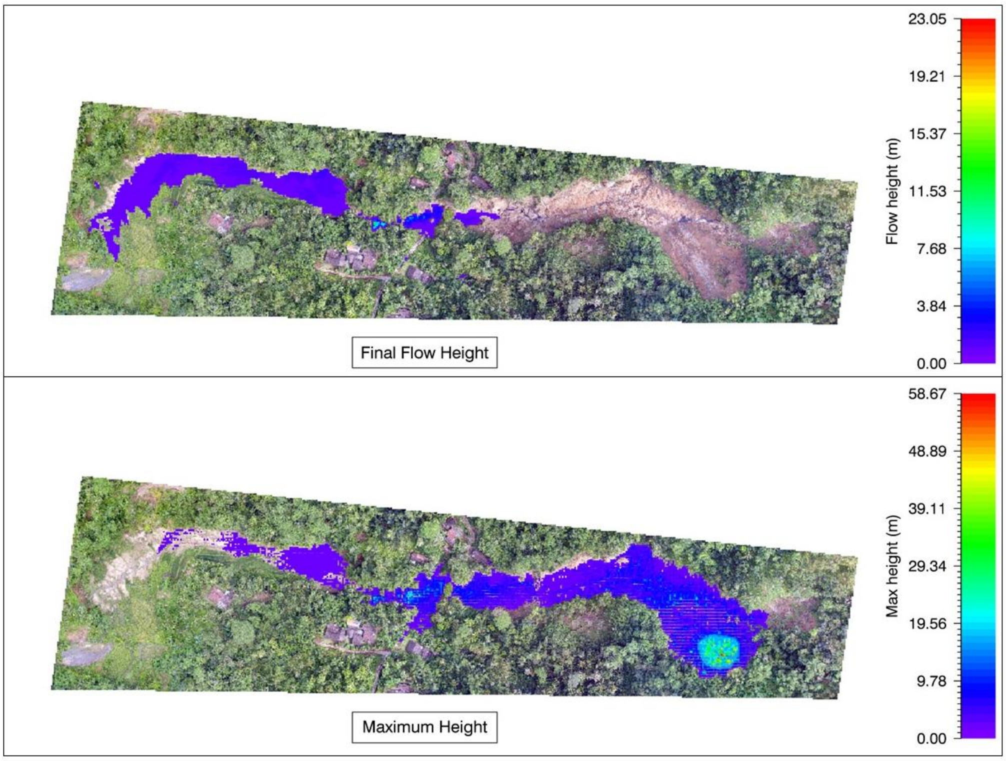

Figure 5.19. Final flow height (above) and maximum flow height (below) of second debris flow

5.2.1.3 Third Debris Flow

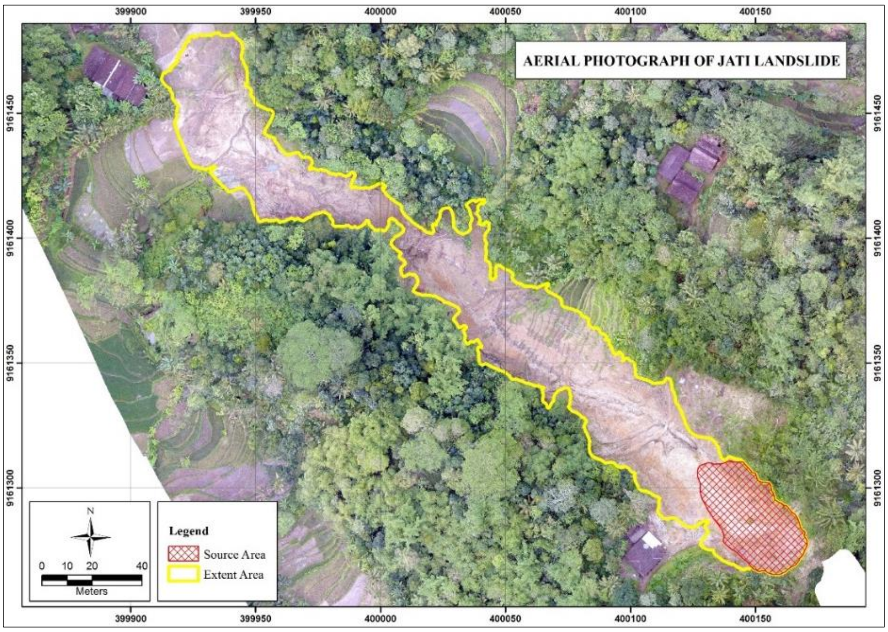

Figure 5.20. Aerial photo of third debris flow

As same as the previous two debris flow events, the third debris flow also occurred on 9 November 2016 around 4 PM due to the extensive rainfall. Due to the debris flow occurrence, high damages are perceived on 0,9 ha agricultural areas especially in the paddy field. Near to the source area, one house was destroyed and some houses were threatened due to the occurrence.

The debris flow has 7,5 m release height with 261,75 m^2 extent area which located at 479,697 m altitude and 30,92° slope. By the result, 2824,72 m^3 material spread from the source area. Those release information was used for input data in the modelling process.

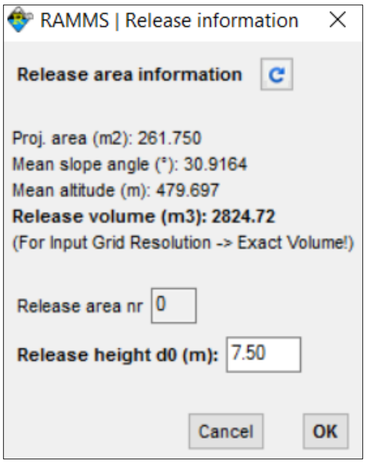

Figure 5.21. Release information of third debris flow

Beside release information, some parameters are also needed for input data of the model. The grid resolution, the end time and sump step value are chosen based on the result expected from the modelling. On the other hands, other parameters are chosen based on soil laboratory analysis and literature review. Based on laboratory tests, the soil in third debris flow is classified as well graded sand which has density (ρ) about 1850 kg/m^3, earth pressure coefficient (λ) about 0,3 , 200 viscous turbulent friction (ξ), 0,65 dry coulomb friction (μ) and 0 cohesion (c).

Table 5.15. Parameters value of third debris flow

	Parameters	Value
Simulation parameters	Grid Resolution (m)	1,5
	End time (s)	2000
	Dump step (s)	5
	Density (kg/m^3)	1850
	Earth pressure coefficient	0,30
Friction parameters	Viscous-turbulent friction	200
	Dry-coulomb friction	0,65
	Cohesion	0

After the modelling process was done, some general output are produced, including simulation duration, maximum velocity and maximum flow height. The following table showed the value of each simulation output;

Table 5.16. Output of third debris flow

Output	Value
Simulation duration (s)	1315
Max velocity (m/s)	80,95
Max flow height (m)	17,59

As same as previous debris flow, the third debris flow has high velocity in the beginning of the simulation. In the first 20 seconds, the release material totally collapsed with a velocity around 13 m/s. There is no significant obstacle faced during the flow, however the velocity decreased towards the end of the simulation.

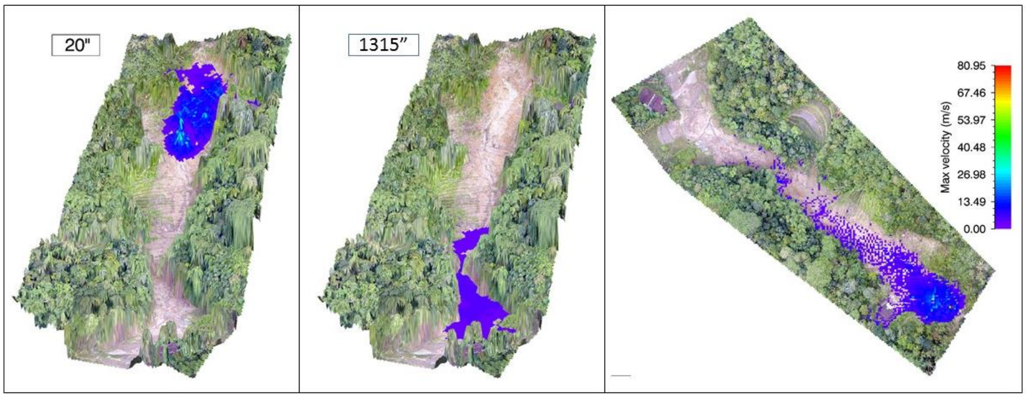

Figure 5.22. Third debris flow simulation (left) and the maximum velocity (right)

In this debris flow, the release area was recorded as the highest maximum height during the simulation. After the release area collapsed, the surrounding area was affected by material spreading which generally have a height not more than 3 meters. Subsequently, the release material flowed to the lower part of the area and totally accumulated in the area with lower elevation.

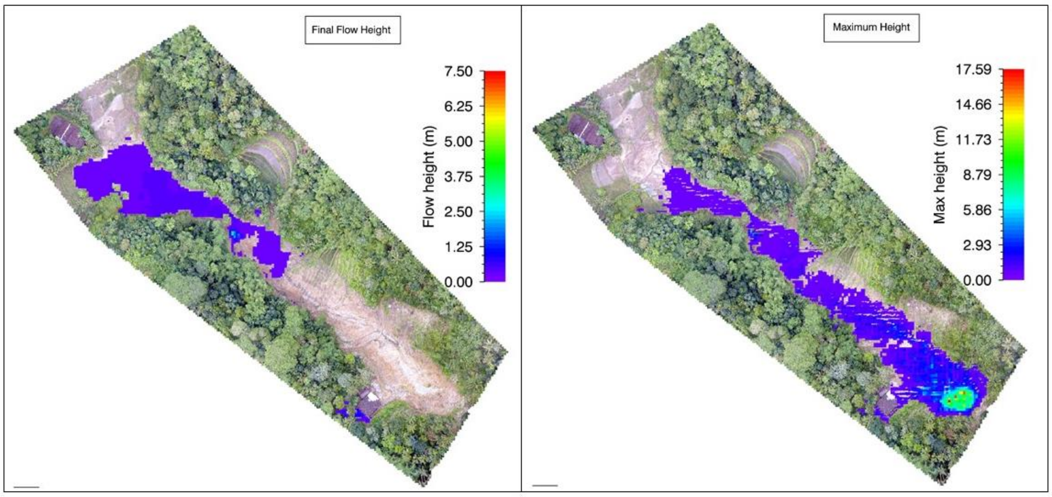

Figure 5.23. Final flow height (left) and maximum flow height (right) of third debris flow

5.2.2 Model Parameterization

Generally, in the modelling, soil property was the main input parameter which determined the result of the simulation. 5 main input parameters were determined by the soil properties, including soil density (ρ), earth pressure coefficient (λ), viscous turbulent friction (ξ), dry coulomb friction (μ) and cohesion (c). Beside determining the soil property of modelled area, analyzing the soil property of small landslide is also applied to specify the input parameters that causing the debris flow. In total there are 3 samples of soil taken from modeled debris flow and 3 samples taken from small landslide. Here is the summary of soil properties from 6 samples taken.

Table 5.17. Soil properties

	Debris flows			Small landslides		
	1st	2nd	3rd	1st	2nd	3rd
USCS	SW-SM	SW	SW	MH	MH	MH
Friction angle	27	33	33	23	23	23
Density	1850	1850	1850	1750	1750	1750
Earth pressure coefficient	0,38	0,3	0,3	0,44	0,44	0,44
Viscous turbulent friction	200	200	200	>200	>200	>200
Dry coulomb-friction	0,51	0,65	0,65	0,42	0,42	0,42
Cohesion	0	0	0	5	5	5

The soil samples were taken from 6 different places, including 3 samples of modelled debris flow events, and 3 samples of small landslides. Based on the sieve analysis and plasticity index analysis, the USCS type of each sample was identified. Generally, debris flows area consist of bigger material compared to it of small landslides. In addition, from the definition of debris flow itself, the debris flow consists of debris which is predominantly coarse. It is impossible that the debris flow consists of fine material such as silt or clay. It was proved by USCS soil type which reported as well graded sand (SW) and well graded sand with silt (SW-SM) for the modelled debris flow samples, whereas high plasticity silt for small landslide samples.

From the material of small landslides, flow type of landslide still possibly happen, but the water content of it must be very high. Or in other words, it will occur in the drainage ways which consist of high water content. This kind of condition will not be named as debris flow but earth flow. In the study area, the area with fine material is not susceptible to flow type landslides since the elevation of small landslides are lower than debris flows.

The soil classification will determine an estimation of the soil friction angle or in other words, the most stable slope of those types of material so there will be no movement in that situation. The finer the material, the smaller the friction angle. Commonly, a certain type of soil will have a range of friction angle, but in this research since it was used for flow modelling, the smaller value was used for input parameter so the flow will reach the runout distance as maximum as possible. In general, the soil which has a smaller friction angle will have longer flow than the soil that has a bigger friction angle. But this friction angle will also determine how much the release volume of the landslide. The higher the friction angle, the greater the amount of release volume from the source area. It is opposite to the small friction angle which will have less release volume from the source area. This fact proved the condition of flow type landslide in the study area.

5.2.2.1 Soil Density (ρ)

According to the study done by (McKenna et al., 2012), which tried to determine the threshold of soil density between the slide type and flow type of landslide, the density was associated with soil porosity and fine-grained content of the material. The combined function of density, porosity and fine content was a good predictor the determined the threshold, while single predictor is not good enough. Nevertheless, single density parameter showed a trend where the higher the density, the more susceptible the area to landside with flow type than slide type.

While in this study, the trend is also similar, which was proved from the soil samples taken from the study area. It showed the debris flow material has a higher density than the density of small landslides. In fact, the density will influence the runout distance of flow material or the type of failure mode whether it is sliding or flowing. It also proved from the definition of the soil density itself, which is the ratio of soil mass with the volume (Black & Blake, 1965). It means the higher the density, the heavier the weight of the soil. Due to driving force from its weight, the sliding or flowing process will be influenced. From the definition of the soil density, it can be concluded that the higher value of density, the more susceptible the soil to flow since the weight of the soil is heavier.

5.2.2.2 Earth Pressure Coefficient (λ)

The earth pressure factor will also influence the flow of landslide material. It indicates the slope resistance to tend the move of its material (Terzaghi, 1943). In the other words, it is the proportion of the vertical and the normal force (Hussin, 2011), which further will influence the flow of landslide material. Since it is related to vertical and normal force, it can be concluded that the earth pressure is associated with friction angle where the higher the friction angle, the lower the earth pressure. Or in other words, the higher the force of the material to flow down the slope, the less the force of the material to the earth.

This fact proved from the soil properties analysis in this study. Based on the result of soil property analysis, the earth pressure of debris flow is lower than small landslide. It indicated that the resistive force of the soil in the debris flow type of landslide is lower than the slide type of landslide. To sum up, the lower the earth pressure, the susceptible the area to flow type of landslide or debris flow.

5.2.2.3 Viscous Turbulent Friction (ξ)

Another input parameter is viscous turbulent friction which represent the flow material, whether it granular or muddy flows (Bartelt et al., 2010). The value for granular flows range between 100 and 200, while the value which higher that 200 represent the muddy flows. The grain size of the soil played the important rule to this parameter. From the soil samples taken, granular particle or coarse particle dominated debris flow material, whereas fine particle dominated small landslide material. For the modelled debris flow value of 200 was chosen since the material was categorized as granular but not really consist of very big grain size material, so the high threshold value was used.

In fact, muddy material has a bigger influence to material flows compared to granular flow. As a result of sensitivity analysis by (Hussin, 2011), the higher the viscous turbulent friction, the longer the runout distance, the higher the deposit volume and the higher the maximum height. The fact that in the Middle Part of Kodil watershed, the debris flow material has lower viscous turbulent compared to small landslide material. It was contradictory with viscous turbulent characteristic in general. This condition indicates that the viscous turbulent friction can not be individual predictor of failure type, the volume of release area might influence the flow. In the study area the volume of the release area in the debris flow event is greater compared to the small landslides.

5.2.2.4 Dry Coulomb Friction (μ)

Aside from the earth pressure coefficient (λ), there is the other parameter that influence by friction angle namely dry coulomb friction. The parameter influences the condition where the flow of material will stop (Bartelt et al., 2010). The value is extracted from the tangent value of the friction angle of the deposition zone. Commonly, the increase of dry coulomb friction value causes the decrease of runout distance (Hussin, 2011).

In this research, the values of dry coulomb friction in small landslides are lower than that in the debris flow. Nevertheless, the runout distance of the debris flow material was higher than the small landslides, which is contradictory to the actual condition. But in fact, if the dry coulomb friction variations are applied to one single debris flow event, it will show the actual condition where the higher the dry coulomb friction, the shorter the debris flow. It is proved that there is no trend of dry coulomb friction value between different landslide events, in contrary the trend was shown within the same landslide event.

5.2.2.5 Soil Cohesion (c)

The last parameter is the cohesion which also obtained from soil property. From soil property analysis, the soil classification was extracted, then by reviewing the literature, a certain value of soil cohesion was obtained. From the analysis, the debris flow material has zero cohesion while small landslides material have 5 cohesion value, which mean the bonds between small landslide material is bigger than debris flow material. The cohesion value influences the stability of the slope as well as the type of mass movement. In this research, the cohesive material which consisted of silt material will move by sliding not by flowing.

Based on the literature, the soils which do not contain clay and silt are low in cohesion or even not cohesive (De Blasio, 2011). The cohesion is linear to the resistive force of a slope where the lower the resistive force compared to gravitational force, the more stable the slope. To sum up, the lower the cohesion, the lower the stability of the slope, or in other words, a long runout landslide such as debris flow might be happened.

5.3 Debris Flow Susceptibility Analysis

Debris flow susceptibility analysis was done by deep analysis of landslide susceptibility as well as debris flow modelling. The parameters causing debris flow from those two sources will be combined to identify the specific parameters causing factor of debris flow. From landslide susceptibility, specific parameter causing debris flow was determined from the certain classes of each parameter which more influential to debris flow occurrence, then furthermore was used to determine the area prone to debris flow. While from debris flow modelling, specific parameters causing debris flow was determined from input parameters of the modelling then subsequently was used to determine the level of susceptibility.

5.3.1 Susceptible Area of Debris Flows

The recorded inventory showed that there were 11 events of debris flow in the study area. Generally, most of the events occurred in the very high classification of landslide susceptibility. Here is the summary of debris flow events and the class of parameters where it occurred.

Table 5.18. Debris flow events based on landslide susceptibility

No	X	Y	Rainfall	Geology	Land use	Landform-Slope	Susceptibility
1	399817	9155118	200-250	Tmoa	Settlement	SM2	Medium
2	398689	9156177	250-300	Tmoa	Plantation	SM3	Medium
3	399134	9159827	250-300	Tmoa	Plantation	SM2	High
4	397417	9162941	250-300	Tmoa	Plantation	D3	High
5	397666	9160222	250-300	Tmoa	Plantation	D3	High
6	398055	9163805	250-300	Tmoa	Plantation	D3	High
7	395521	9162229	250-300	Tmoa	Paddy Field	VS3	Very High
8	394626	9162913	250-300	Tmoa	Paddy Field	VS3	Very High
9	400117	9161284	250-300	Tmoa	Plantation	SM3	Medium
10	398286	9162916	250-300	Tmoa	Plantation	D3	High
11	400531	9162216	200-250	Tmoa	Plantation	SM3	Medium

Based on rainfall parameter, 9 from 11 recorded debris flows occurred in the area with 3 days cumulative rainfall more than 250 mm. It was correlated with the weight that was produced by landslide susceptibility analysis, which highest weight of rainfall, 0,263, was received by that class. On the other hands, the other two events occurred in the area which has 3 days cumulative rainfall around 200 to 250 mm.

The study area is dominated by Tmoa (old andesite formation) geology type which most of landslides as well as debris flow occurred. Not all recorded landslides occurred in this geology class, but all recorded debris flow events occurred in this geology classification. Based on the weight of evidence analysis, this class had the highest weight which is 0,263. It is proved that the most influential geology class which causing landslides is the same as debris flow.

From land use parameter, 8 events was occurred in plantation area, 2 others occurred in the paddy field area, while the other one occurred in the settlement area. It is not equivalent to the weight produced from landslide susceptibility analysis since highest weight was received by paddy field with 1,091 value. Nevertheless, the plantation was placed in the second order of the weight after paddy field with -0,285 weight. However, based the fieldwork experience, the initiation area of debris flow occurred in the plantation, but then the material flowed into the paddy field area. It occurred since the paddy field area was commonly associated with plantation area and has a significant elevation difference with plantation area. Or in other words, plantation with steep slope are susceptible to debris flow when it is located next to the paddy field area which located in the valley.

The last parameter is a combination of landform and slope. From the recorded data it was shown that the debris flows occurred in many different combinations of landform and slope including structural, volcanic and denudational with 15 to 45 % slope area. The denudational landform with 25 to 45% slope is the widest area where the debris flow occurred. It happened since the denudational area was prone to erode or in other words, it is not as stable as other landforms. The combination with 25 to 45% slope also increases the level of susceptibility to the debris flow. Based on the weight of evidence analysis of the landslide, the weight of this kind of landform-slope combination was the highest weight among other combinations. Besides occurred in denudational landform, debris flow also frequently occurred to structural landform with 2 different classes of slope including 15 to 25% and 25 to 45%. Moreover, another combination where the debris flow occurred is the volcanic landform with 25 to 45% slope.

From the weight of evidence analysis of landslide susceptibility, it is can be concluded that the susceptible area to debris flow is almost the same to landslide susceptibility. It was proved by the weight values of the specific parameters which are the highest value compared to other classes. From the analysis, it can be concluded that in the study area, the debris flow susceptibility is high in plantation area which located in old andesite formation and denudational area with 25 to 45% slope when triggered by more than 250 mm 3 days cumulative rainfall.

5.3.2 Level of Debris Flows Susceptibility

To make the precise debris flow susceptibility analysis, the modelling was used to improve specific parameters causing debris flow, which previously has been analyzed from landslide susceptibility analysis. The modelling was done using back analysis in the area where the debris flow have been occurred. The model parameters was calibrated until the debris flow extent in the simulation is similar to the actual extent. By all those model parameters, it can be concluded that debris flow will occur in the area which has a big grain size of the soil such as sand or gravel which has a high density (ρ), in other hand it have small earth pressure coefficient (λ), viscous turbulent friction (ξ), dry coulomb friction (μ) and cohesion (c).

Table 5.19. The influence of input parameters to debris flow susceptibility

	Debris Flow Susceptibility
	high → low
Soil density	high → low
Earth pressure	low → high
Viscous turbulent	low → high
Dry coulomb friction	low → high
Cohesion	low → high

5.3.3 Summary of Debris Flows Susceptibility

Finally, according to the debris flow analysis resulted from landslide susceptibility and debris flow modelling, it can be summarized that the area prone to debris flow and its level can be determined. The area prone to debris flow could be extracted from the specific parameters produced by landslide susceptibility analysis, while the level of debris flow susceptibility could be extracted from debris flow input parameter. For the prone area of debris flow, it is a must that the area should meet all criteria in the following table.

Table 5.20. Summary of debris flows susceptibility analysis

Susceptibility area to debris flow determination	**Level of debris flow susceptibility determination**
1. The area must have 3 days cumulative rainfall intensity more than 250 mm 2. The area must be in Tmoa geological class 3. The area must be on a plantation or paddy field area 4. The area must have 25 to 45% slope or 15 to 25 % slope under structural landform	1. The higher the density (ρ) the more susceptible to debris flow 2. The lower the earth pressure coefficient (λ) the more susceptible to debris flow 3. The lower the viscous turbulent friction (ξ), the more susceptible the area to debris flow 4. The lower the dry coulomb friction (μ), the more susceptible the area to debris flow 5. The lower the cohesion (c), the more susceptible the area to debris flow.

By the result that have already been obtained it is possible to determine the area susceptible to debris flow yet on the other hands, determining the level of debris flow susceptibility will be difficult since the parameter of level determination is very specific. The specific soil map is needed to construct the level of debris flow susceptibility.

CHAPTER 6. CONCLUSIONS AND RECOMMENDATIONS

6.1 Conclusions

After the research was done, seven points of conclusion were obtained to answer the research question;

1. The landslide susceptibility map was built by using weight of evidence analysis, which involved 4 parameters including rainfall, geology formation, land use and combination of landform and slope. Those parameters are the general factor causing landslides.
2. The level of landslide susceptibility showed the correlation with the inventory data. It was proved by the high landslide susceptibility level in the middle of the study area where most of the recorded landslide events occurred.
3. Based on landslide susceptibility analysis, the specific parameters causing debris flow are 3 days cumulative rainfall more than 250 mm, old andesite geology formation, plantation and paddy field area, all landform classes with 25 to 45% slope added by structural landform which has 15 to 25% slope.

   Those specific parameters were generated based on the factual reasons. The higher the rainfall, the more susceptible the instability of the slope. Then in fact the old andesite is the widest geological formation in the study area, so that this class will dominate the debris flow occurrence, yet there is scientific reason of landslide occurrence in this area. It was because it formed by the volcanic activities which is prone to weather, then prone to slope instability. Commonly the extensive land use change is the main cause of paddy filed become the specific parameter causing debris flow. The paddy field, which was cultivated on a slope area, will cause the instability of the slope, due to the treatment of the area is higher than previous land use. Besides, the plantation which next to paddy field will also face the effect of the instability. Different landforms will have different stability even in the same slope class, it was showed from structural landform which prone in 15 to 25% slope. It happened because the structural landform consist of clear dip and strike which easily to fail even in the gentle slope.

4. The first debris flow simulation finished in 4 minutes with 18,1m/s maximum velocity and 16,1 m maximum flow height. Furthermore, the second debris flow was the longer simulation which ended in 1 hour and 6 minutes, with 149,95 m/s maximum velocity and 58,67 m flow height. Then the last debris flow was end 22 minutes with 80,95 m/s maximum velocity and 17,59 m flow height.

   The simulation result showed the significant differences in the second debris flow, it was because the release volume and the release slope of the second debris flow was higher compared to the other two. Therefore the the second debris flow velocity was higher than others. Even the velocity was the highest, the simulation time of the second debris flow was the longest compared to other debris flow. It happened because the topography of the area formed a slit in a certain part, so that the velocity was reduced, then causing the long simulation time. Besides, it also affected the height of the flow, which was the higher among the other two debris flows.

5. There are 5 input parameters of modelling that influence the debris flow such as soil density (ρ), earth pressure coefficient (λ), viscous turbulent friction (ξ), dry coulomb friction (μ) and cohesion (c). The higher the soil density (ρ), the higher the susceptibility to debris flow. In contrary, the higher the earth pressure coefficient (λ), viscous turbulent friction (ξ), dry coulomb friction (μ) and cohesion (c), the lower the debris flow susceptibility.

   From the result obtained, instead of determining the debris flow occurrence, those parameters give much influence to the movement of the debris flow, especially the magnitude of the flow. All the parameters influencing the movement of debris flow, such as the extent area, the velocity, the flow height and the duration of the simulation.

6. The specific parameters causing debris flow, which produced by landslide susceptibility (point 3) can be used to determine area susceptible to the debris flow by overlapping all parameters. Whereas to determine the level of debris flow susceptibility, the modelling calibrated input parameters (point 5) can be used.

   Based on the result obtained, the susceptible area of debris flow was only can be determined using landslide susceptibility analysis, yet the parameters from debris flow modelling only influenced the magnitude of the flow. So that the area prone to debris flow was generated from parameters produced by landslide susceptibility. Then the parameters from debris flow modelling was used to determine the class or the level of debris flow susceptibility and is not used to determine the specific area prone to debris flow.

7. It is possible to determine the area of debris flow susceptibility, yet the class or the level of susceptibility distribution in the area is difficult to determine, because it needs detailed maps of soil physical parameters to construct the parameters map. Besides, the potential runout area was also could not be determined.

6.2 Recommendations

Based on research result, some recommendation are recommended, including:

1. The landslide inventory about the size and the absolute location sometimes was still subjectively constructed since the ability of local authority to read imagery and to recall the previous event is limited. The deep participatory mapping is needed to get more accurate data.
2. More detail rainfall data should be taken into account to get more realistic susceptibility information. Collecting rainfall data or interpolation method should be improved.
3. Because the complexity of the debris flow occurrence, many influential factors that not included in landslide susceptibility analysis and debris flow modelling. So, in further research, including other physical factors which obtain from fieldwork experience is recommended to get a better analysis.
4. Further research concerning about constructing the detailed maps of soil physical parameters resulted from debris flow modelling can be done. It is necessary to construct the debris flow susceptibility map.

5. The further research about determining the threshold of model input parameters that influencing the magnitude of debris flow is suggested for further research to obtain specific class of debris flow susceptibility.
6. Further study is needed on a potential runout area of debris flow so the susceptible area of debris flow was not only generated from potential area to fail becoming debris flow, but also the prone area to be covered by debris flows.

REFERENCE

Agisoft photoscan user manual. (2011) (Proffesion). St. Petersburg, Russia: Agisoft LCC.

Arnous, M. O. (2010). Integrated remote sensing and GIS techniques for landslide hazard zonation: a case study Wadi Watier area, South Sinai, Egypt. *Journal of Coastal Conservation*, *15*(4), 477–497. http://doi.org/10.1007/s11852-010-0137-9

Barbieri, G., & Cambuli, P. (2009). The weight of evidence statistical method in landslide susceptibility mapping of the Rio Pardu Valley (Sardinia, Italy). *18th World IMACS / MODSIM Congress*, 2658–2664. Retrieved from http://mssanz.org.au/modsim09

Bartelt, P., Buehler, Y., Christen, M., Deudelbeiss, Y., Graf, C., McArdell, B., … Schneider, M. (2010). *RAMMS, user manual debris flow* (V1.5). Swiss: WSL Institute for Snow and Avalanche Research SLF.

Bemmelen, R. W. Van. (1949). *Geology of Indonesia*. The Hague: Goverment Printing Office.

Black, C. A., & Blake, G. R. (1965). Bulk density. In *Methods of soil analysis. part 1. physical and mineralogical properties, including statistics of measurement and sampling* (pp. 374–390). Madison: American Society of Agronomy, Soil Science Society of America.

Blahut, J., Horton, P., Sterlacchini, S., & Jaboyedoff, M. (2010). Debris flow hazard modelling on medium scale: Valtellina di Tirano, Italy. *Natural Hazards and Earth System Science*, *10*(11), 2379–2390. http://doi.org/10.5194/nhess-10-2379-2010

Blahut, J., Klimes, J., & Varilova, S. (2013). Quantitative rockfall hazard and risk analysis in selected municipalities of the Ceske Svycarsko National Park, Northwestern Czechia. *Geografie*, *118*(3), 205–220. Retrieved from https://www.researchgate.net/profile/Jan_Klimes/publication

BNPB. (n.d.). Data dan informasi bencana Indonesia. Retrieved from http://dibi.bnpb.go.id/

Cesca, M., & D’Agostino, V. (2008). Comparison between FLO-2D and RAMMS in debris-flow modelling: A case study in the Dolomites. *WIT Transactions on Engineering Sciences*, *60*, 197–206. http://doi.org/10.2495/DEB080201

Chambers, R. (2006). Participatory mapping and geographic information systems: whose map? Who is empowered and who disempowered? Who gains and who loses? *The Electronic Journal of Information Systems in Developing Countries*, *25*(2), 1–11. http://doi.org/144.214.55.140

Chen, H., & Lee, C. F. (2004). Geohazards of slope mass movement and its prevention in Hong Kong. *Engineering Geology*, *76*(1–2), 3–25. http://doi.org/10.1016/j.enggeo.2004.06.003

Christen, M., Bartelt, P., Kowalski, J., & Stoffel, L. (2008). Calculation of dense snow avalanches in three-dimensional terrain with the numerical simulation program ramms. *International Snow Science Workshop*, 709–716. Retrieved from http://ramms.slf.ch/ramms

Christen, M., Bühler, Y., Bartelt, P., Leine, R., Glover, J., Schweizer, A., … Feistl, T. (2012). Integral hazard management using a unified software environment numerical simulation tool " Ramms ." *12th Congress Interpraevent*, 77–86. Retrieved from http://www.interpraevent.at

Christen, M., Kowalski, J., & Bartelt, P. (2010). RAMMS: Numerical simulation of dense snow avalanches in three-dimensional terrain. *Cold Regions Science and Technology*, *63*(1–2), 1–14. http://doi.org/10.1016/j.coldregions.2010.04.005

De Blasio, F. V. (2011). Friction, cohesion, slope stability. In *Introduction to the physics of landslides* (pp. 23–52). Netherlands: Springer.

Feizizadeh, B., Shadman Roodposhti, M., Jankowski, P., & Blaschke, T. (2014). A GIS-based extended fuzzy multi-criteria evaluation for landslide susceptibility mapping. *Computers & Geosciences*, *73*, 208–221. http://doi.org/10.1016/j.cageo.2014.08.001

Fell, R., Corominas, J., Bonnard, C., Cascini, L., Leroi, E., & Savage, W. Z. (2008). Guidelines for landslide susceptibility, hazard and risk zoning for land use planning. *Engineering Geology*, *102*(3–4), 85–98. http://doi.org/10.1016/j.enggeo.2008.03.022

Guo, D., Hamada, M., He, C., Wang, Y., & Zou, Y. (2014). An empirical model for landslide travel distance prediction in wenchuan earthquake area. *Landslides*, *11*(2), 281–291. http://doi.org/10.1007/s10346-013-0444-y

Hervas, J. (2013). Landslide inventory. In *Encyclopedia of natural hazards* (pp. 610–611). Berlin: Springer.

Hungr, O., Evans, S. G., Bovis, M. J., & Hutchinson, J. N. (2001). A review of the classification of landslides of the flow type. *Environmental & Engineering Geoscience*, *VII*(3), 221–238. http://doi.org/10.2113/gseegeosci.7.3.221

Hussin, H. Y. (2011). *Probabilistic run-out modeling of a debris flow in Barcelonnette , France*. MSc Thesis, University of Twente.

Ishibashi, I., & Hazarika, H. (2011). *Soil mechanics fundamentals*. Boca Raton, Florida: CRC Press.

Karnawati, D. (1998). Natural Slope Failure on Weathered Andesitic Breccia in Samigaluh Area, Indonesia. *International Conference on Case Histories in Geotechnical Engineering*, *14*, 495–501. Retrieved from http://scholarsmine.mst.edu/icchge/

Kritikos, T., & Davies, T. (2014). Assessment of rainfall-generated shallow landslide/debris-flow susceptibility and runout using a GIS-based approach: application to western Southern Alps of New Zealand. *Landslides*, (February), 1051–1075. http://doi.org/10.1007/s10346-014-0533-6

Mair, A., & Fares, A. (2011). Comparison of rainfall interpolation methods in a mountainous region of a tropical island. *Journal of Hydrologic Engineering*, *16*(4), 371–383. http://doi.org/10.1061/(ASCE)HE.1943-5584.0000330

Mandaglio, M. C., Gioffrè, D., Pitasi, A., & Moraci, N. (2016). Qualitative landslide susceptibility assessment in small areas. *Procedia Engineering*, *158*, 440–445. http://doi.org/10.1016/j.proeng.2016.08.469

Martha, T. R. (2012). Synergetic use of satellite image and DEM for identification of landforms in a ridge-valley topography. *International Journal of*

Geosciences, *3*(3), 480–489. http://doi.org/10.4236/ijg.2012.33051

McKenna, J. P., Santi, P. M., Amblard, X., & Negri, J. (2012). Effects of soil-engineering properties on the failure mode of shallow landslides. *Landslides*, *9*(2), 215–228. http://doi.org/10.1007/s10346-011-0295-3

Nettleton, I. M., Martin, S., Hencher, S., & Moore, R. (2005). Debris flow types and mechanisms. *Scottish Road Network Landslides Study*, (August), 1–119. Retrieved from http://www.scotland.gov.uk/Publications/2005/07/08131738/17395

Peres, D. J., & Cancelliere, a. (2014). Derivation and evaluation of landslide triggering thresholds by a Monte Carlo approach. *Hydrol. Earth Syst. Sci. Discuss.*, *11*(2007), 2759–2794. http://doi.org/10.5194/hessd-11-2759-2014

Phantom 4 - user manual. (2016) (V1.0). Colombia: Heliboss.

Quan Luna, B. (2012). *Dynamic numerical run - out modelling for quantitative landslide risk assessment*. Doctoral dissertation, University of Twente.

Quan Luna, B., Blahut, J., Camera, C., van Westen, C., Apuani, T., Jetten, V., & Sterlacchini, S. (2013). Physically based dynamic run-out modelling for quantitative debris flow risk assessment: a case study in Tresenda, northern Italy. *Environmental Earth Sciences*, *72*(3), 645–661. http://doi.org/10.1007/s12665-013-2986-7

Rusdiyatmoko, A. (2013). *Incorporating landslide susceptibility in land rehabilitation*. MSc Thesis, University of Twente.

Sassa, K., Fukuoka, H., Wang, F., & Wang, G. (2007). *Progress in landslide science*. Berlin: Springer Verlag.

Scheuner, T., Schwab, S., & Mcardell, B. W. (2011). Application of a two-dimensional numerical model in risk and hazard assessment in Switzerland. *5th DFHM*, 993–1001. http://doi.org/10.4408/IJEGE.2011-03.B-108

Schraml, K., Thomschitz, B., Mcardell, B. W., Graf, C., & Kaitna, R. (2015). Modeling debris-flow runout patterns on two alpine fans with different dynamic simulation models. *Natural Hazards and Earth System Sciences*, *15*(7), 1483–1492. http://doi.org/10.5194/nhess-15-1483-2015

Song, R. H., Hiromu, D., Kazutoki, A., Usio, K., & Sumio, M. (2008). Modeling the potential distribution of shallow-seated landslides using the weights of evidence method and a logistic regression model: a case study of the Sabae Area, Japan. *International Journal of Sediment Research*, *23*(2), 106–118. http://doi.org/10.1016/S1001-6279(08)60010-4

Subramanian, N. (2008). *Design of steel Structures*. *Oxford University Press*. India: Oxford University Press, India.

Swanson, F. J., Kratz, T. K., Caine, N., & Woodmansee, R. G. (1988). Landform effects on ecosystem patterns and processes. *BioScience*, *38*(2), 92–98. http://doi.org/10.2307/1310614

Terzaghi, K. (1943). *Theoretical soil mechanics*. New York, London: John Wiley and Sons, inc.

Van Westen, C. J. (2002). *Use of weights of evidence modeling for landslide susceptibility mapping* (Class Hand). Retrieved from https://rdc.blackboard.com

Varnes, D. J. (1978). Slope movement types and processes. In *Special report 176:*

landslides: analysis and control (pp. 11–33). Washington D. C: Transportation and Road Research Board, National Academy of Science.

Varnes, D. J. (1984). *The principles and practice of landslide hazard zonation*. France: Unesco.

Vescovi, P. (2006). A GIS-based automated procedure for landslide susceptibility mapping by the conditional analysis method : the Baganza valley case study (Italian Northern Apennines). *Environmental Geologogy*, *50*, 941–961. http://doi.org/10.1007/s00254-006-0264-7

Zhang, Y. J., Chen, L. Z., Xing, A. G., & Qi, C. (2013). Dynamic Simulation and Analysis of High-Speed and Long Run-Out Landslide Triggered by the Wenchuan Earthquake, China. *Earthquake-Induced Landslides*, 567–574. http://doi.org/10.1007/978-3-642-32238-9

APPENDIX

Appendix 1. Documentations

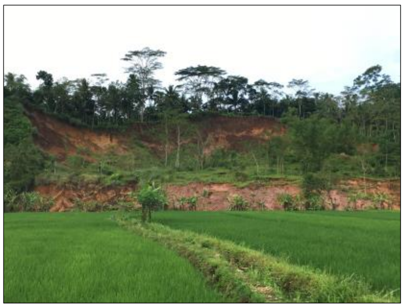
Landslide in the study area


Damage caused by debris flow


First debris flow


Second debris flow


Third debris flow


Soil sample taking


Soil sample of landslide


Soil sample of debris flow

Appendix 2. Landslide Inventory

No	Time			Location					Coordinate		Slope	Length	Width
	Year	Month	Day	Subdistrict	Village	Hamlet	RT	RW	X	Y			
1	2003	February	0	Salaman	Margoyoso	Blok Nlongo	0	0	110,0825	-7,5706	25	90	30
2	2003	February	0	Bener	Wadas		0	0	110,0777	-7,6357	20	70	23
3	2003	February	1	Bener	Kaliwader	Ngabean	4	2	110,0979	-7,6409	27	30	21
4	2003	February	1	Bener	Kaliwader	Kalilepang 1	2	2	110,0905	-7,6424	13	4	2
5	2003	February	1	Bener	Kaliwader	Kalilepang 1	2	2	110,0910	-7,6425	17	4	2
6	2004	January	0	Bener	Kaliwader	Ngabean	4	2	110,0979	-7,6417	15	20	20
7	2004	January	0	Bener	Kaliwader	Kalilepang 1	2	2	110,0917	-7,6425	11	150	20
8	2005	January	0	Bener	Wadas		0	0	110,0815	-7,6329	18	200	11
9	2006	January	0	Bener	Jati		0	0	110,0856	-7,5999	14	250	82
10	2006	January	0		Legetan	Blok Munggang	0	0	110,0455	-7,5982	15	8	4
11	2006	January	0	Bener	Sukowuwuh	Merati	1	1	110,0421	-7,5819	10	34	6
12	2006	January	1	Bener	Ketosari	Kedung Agung	2	2	110,0577	-7,5972	16	5	5
13	2006	January	1	Bener	Ketosari	Kedung Agung	1	2	110,0645	-7,5988	10	50	20
14	2006	January	1	Bener	Kalijambe	Sikembang	3	2	110,0637	-7,5840	24	18	13
15	2006	January	1	Bener	Kalijambe	Sikembang	2	2	110,0656	-7,5859	19	9	3
16	2006	January	1	Bener	Kalijambe	Sikembang	2	2	110,0659	-7,5858	8	13	10
17	2006	January	1	Bener	Kalijambe	Gamblok	3	1	110,0651	-7,5920	18	6	3
18	2006	January	1	Bener	Kalijambe	Gamblok	3	1	110,0668	-7,5904	15	42	19
19	2006	January	1	Bener	Kalijambe	Gamblok	1	1	110,0710	-7,5899	13	20	13
20	2006	January	1	Bener	Mayungsari		0	0	110,0910	-7,5701	16	100	12
21	2006	January	1	Bener	Mayungsari	Krajan 2	4	2	110,0970	-7,5781	15	15	7
22	2006	January	1	Bener	Mayungsari	Palal	3	2	110,0973	-7,5763	13	78	18

No	Time			Location					Coordinate		Slope	Length	Width
	Year	Month	Day	Subdistrict	Village	Hamlet	RT	RW	X	Y			
23	2006	January	1	Bener	Mayungsari	Palal	3	2	110,0972	-7,5773	18	11	8
24	2006	January	1	Bener	Mayungsari	Ngipik	1	2	110,0893	-7,5770	8	19	10
25	2006	January	1	Bener	Mayungsari	Ngipik	1	2	110,0903	-7,5772	6	15	12
26	2006	January	1	Bener	Medono	Lemah Abang	2	2	110,0897	-7,6017	25	33	6
27	2006	January	1	Bener	Ketosari	Kedung Agung	1	2	110,0567	-7,5923	32	40	20
28	2006	January	1	Bener	Ketosari	Kedung Agung	1	2	110,0598	-7,5979	16	3	7
29	2006	January	1	Bener	Ketosari	Kedung Agung	1	1	110,0614	-7,6085	30	13	8
30	2007	April	0	Bener	Kamijoro	Krajan	2	2	110,0684	-7,6053	16	5	3
31	2007	April	20	Bener	Kalijambe	Mantenan	2	5	110,0717	-7,5732	17	11	7
32	2008	March	0		Pekacangan		0	0	110,0929	-7,6114	6	30	11
33	2008	March	0	Bener	Wadas		0	0	110,0839	-7,6246	15	50	23
34	2008	March	0	Bener	Wadas		0	0	110,0913	-7,6262	24	25	8
35	2008	March	0	Bener	Kamijoro	Ngemplak	3	3	110,0723	-7,6036	14	7	6
36	2008	March	9	Bener	Kalitapas		0	0	110,1088	-7,6243	30	4	3
37	2009	January	30	Bener	Mayungsari	Krajan 2	4	2	110,0924	-7,5793	26	90	42
38	2009	February	0	Bener	Kamijoro	Krajan	1	2	110,0677	-7,6022	17	5	5
39	2009	February	0	Bener	Kamijoro		0	0	110,0703	-7,5997	9	6	5
40	2009	February	0	Bener	Kamijoro	Krajan	1	1	110,0723	-7,5963	25	200	86
41	2009	February	2	Bener	Medono	Ngaglik	1	2	110,0917	-7,6007	16	14	10
42	2009	February	2	Bener	Medono	Krajan	1	2	110,0943	-7,6059	15	7	3
43	2009	February	5	Bener	Kalijambe	Mantenan	2	5	110,0686	-7,5730	28	30	13
44	2009	February	5	Bener	Kalijambe	Mantenan	2	5	110,0701	-7,5717	23	120	30
45	2009	February	5	Bener	Kalijambe	Mantenan	2	5	110,0657	-7,5745	12	4	2
46	2009	February	5	Bener	Kalijambe	Sorogenen	1	4	110,0726	-7,5887	16	13	8

No	Time			Location					Coordinate		Slope	Length	Width
	Year	Month	Day	Subdistrict	Village	Hamlet	RT	RW	X	Y			
47	2009	February	5	Bener	Kalijambe	Gamblok	1	3	110,0648	-7,5916	23	60	20
48	2009	February	5	Bener	Kalijambe	Gamblok	1	2	110,0650	-7,5910	12	7	5
49	2009	February	5	Bener	Kalijambe	Sikembang	2	2	110,0656	-7,5859	20	10	6
50	2009	February	5	Bener	Kalijambe	Sikembang	2	2	110,0659	-7,5858	8	13	10
51	2009	February	5	Bener	Kalijambe	Bendo	3	1	110,0665	-7,5861	15	19	4
52	2009	February	5	Bener	Kalijambe	Mantenan	2	5	110,0658	-7,5744	12	2	1
53	2009	February	5	Bener	Kalijambe	Sikembang	2	2	110,0780	-7,5858	15	31	10
54	2009	February	5	Bener	Kalijambe	Sikembang	2	2	110,0667	-7,5862	5	3	2
55	2009	February	5	Bener	Kalijambe	Sikembang	2	2	110,0699	-7,5886	17	10	5
56	2009	March	0	Bener	Kamijoro	Krajan	3	2	110,0638	-7,6074	9	41	22
57	2010	January	0	Salaman	Margoyoso		0	0	110,0661	-7,5622	12	30	10
58	2010	January	24	Bener	Jati	Kembangan Lor	2	4	110,0847	-7,5906	25	9	5
59	2010	March	19	Bener	Ketosari	Kebun Legi	4	1	110,0606	-7,6089	28	24	10
60	2010	December	0		Pekacangan		0	0	110,0914	-7,6109	8	17	6
61	2010	December	0		Pekacangan		0	0	110,0971	-7,6128	16	17	9
62	2010	December	0		Pekacangan		0	0	110,0958	-7,6158	30	47	43
63	2010	December	0		Pekacangan		0	0	110,1012	-7,6070	25	41	17
64	2010	December	0		Nglaris		0	0	110,0336	-7,5644	29	80	50
65	2010	December	0	Bener	Bleber		0	0	110,0822	-7,6109	29	88	52
66	2010	December	6	Bener	Jati		0	0	110,0865	-7,5885	26	20	9
67	2010	December	6	Bener	Jati		0	0	110,0836	-7,5957	25	2	2
68	2011	February	28	Bener	Jati	Siringin	1	7	110,0915	-7,5858	18	19	16
69	2011	March	20		Nglaris		2	4	110,0264	-7,5729	9	37	7
70	2011	March	20		Nglaris		2	4	110,0261	-7,5747	14	6	5

No	Time			Location					Coordinate		Slope	Length	Width
	Year	Month	Day	Subdistrict	Village	Hamlet	RT	RW	X	Y			
71	2011	November	29	Bener	Kaliwader	Ngabean	4	2	110,0974	-7,6422	23	4	4
72	2011	November	29	Bener	Kaliwader	Kalilepang 1	2	2	110,0894	-7,6432	9	2	1
73	2011	November	29	Bener	Kaliwader	Ringinsari	4	1	110,0838	-7,6435	11	9	4
74	2011	November	29	Bener	Kaliwader	Kalilepang II	3	2	110,0946	-7,6426	32	5	4
75	2011	November	29	Bener	Kaliwader	Kalilepang 1	2	2	110,0883	-7,6432	12	10	4
76	2011	November	29	Bener	Kaliwader	Ngabean	4	2	110,0975	-7,6423	23	2	1
77	2011	November	29	Bener	Kaliwader	Kalilepang 1	2	2	110,0889	-7,6432	9	3	1
78	2011	November	29	Bener	Kaliwader	Kalilelapang	4	2	110,0976	-7,6422	23	2	1
79	2011	November	29	Bener	Kaliwader	Kalilepang II	3	2	110,0949	-7,6426	30	2	2
80	2011	November	29	Bener	Kaliwader	Ngabean	4	2	110,0974	-7,6417	24	3	1
81	2011	November	29	Bener	Kaliwader	Ngabean	4	2	110,0974	-7,6420	23	3	1
82	2011	November	29	Bener	Cacaban Lor	Kemiri Sewu	1	3	110,1096	-7,6178	30	10	3
83	2011	November	29	Bener	Cacaban Lor	Kemiri Sewu	2	3	110,1091	-7,6160	15	10	8
84	2011	November	29	Bener	Kalitapas		0	0	110,1009	-7,6405	31	24	16
85	2011	December	0	Bener	Sokowuwuh	Pandak	1	5	110,0505	-7,5862	25	37	30
86	2011	December	0		Nglaris		0	0	110,0393	-7,5555	15	82	34
87	2011	December	20	Bener	Ketosari	Kedung Agung	1	2	110,0552	-7,5964	23	18	7
88	2011	December	20	Bener	Ketosari	Kedung Agung	2	2	110,0555	-7,5967	24	22	9
89	2011	December	20	Bener	Ketosari	Kedung Agung	1	2	110,0583	-7,5925	31	4	2
90	2011	December	20	Bener	Cacaban Lor	Kemiri Sewu	1	3	110,1086	-7,6181	10	11	5
91	2011	December	20	Bener	Cacaban Lor	Pending	2	2	110,1080	-7,6168	9	11	8
92	2011	December	20	Bener	Kalijambe	Sikembang	1	2	110,0703	-7,5882	8	6	6
93	2011	December	20	Bener	Kalijambe	Mantenan	2	5	110,0685	-7,5726	22	39	26
94	2011	December	20	Salaman	Margoyoso	Sabrang	7	4	110,0758	-7,5675	18	50	42

No	Time			Location					Coordinate		Slope	Length	Width
	Year	Month	Day	Subdistrict	Village	Hamlet	RT	RW	X	Y			
95	2011	December	20	Salaman	Margoyoso	Tubansari	1	6	110,0759	-7,5639	22	182	121
96	2011	December	20	Salaman	Margoyoso	Tubansari	5	6	110,0699	-7,5615	19	28	12
97	2011	December	20	Salaman	Margoyoso	Tubansari	4	6	110,0699	-7,5639	17	14	13
98	2011	December	20	Salaman	Margoyoso	Kalisari	4	5	110,0680	-7,5675	34	11	3
99	2011	December	20	Salaman	Margoyoso	Kalisari	3	5	110,0693	-7,5677	27	7	4
100	2011	December	20	Salaman	Margoyoso	Kalisari	2	5	110,0700	-7,5676	22	7	3
101	2011	December	20	Salaman	Margoyoso	Tubansari	1	6	110,0761	-7,5652	18	76	27
102	2011	December	20	Salaman	Margoyoso	Tlogosari	2	3	110,0813	-7,5685	9	42	26
103	2012	January	0		Legetan	Blok Panditan Barat	0	0	110,0338	-7,5946	24	47	24
104	2012	January	0		Legetan	Blok Panditan Selatan	0	0	110,0366	-7,5973	31	2	2
105	2012	January	1	Bener	Ketosari	Kedung Agung	1	2	110,0595	-7,6099	33	10	1
106	2012	January	1	Bener	Ketosari	Kedung Agung	2	2	110,0591	-7,5972	12	24	15
107	2012	January	1	Bener	Kalijambe	Bendo	1	3	110,0717	-7,5850	31	41	29
108	2012	January	1	Bener	Mayungsari	Ngipik	1	2	110,0912	-7,5783	18	50	34
109	2012	January	1	Bener	Mayungsari	Depok	3	2	110,0815	-7,5791	19	6	5
110	2012	January	1	Bener	Mayungsari	Santren	5	1	110,0853	-7,5783	25	14	10
111	2012	January	1	Bener	Sokowuwuh	Balimangu	1	2	110,0408	-7,5698	25	9	7
112	2012	January	1	Bener	Sokowuwuh	Balimangu	2	2	110,0423	-7,5699	17	7	4
113	2012	January	1	Bener	Sokowuwuh	Krajan	1	3	110,0521	-7,5774	22	50	14
114	2012	January	1	Bener	Sokowuwuh	Krajan	1	3	110,0523	-7,5776	27	8	4
115	2012	January	1	Bener	Sokowuwuh	Krajan	1	3	110,0517	-7,5778	22	19	18
116	2012	January	1	Bener	Sokowuwuh	Watubelah	1	4	110,0543	-7,5756	38	10	5
117	2012	January	1	Bener	Sokowuwuh	Pandak	2	5	110,0523	-7,5876	13	22	15
118	2012	January	1	Bener	Sokowuwuh	Watubelah Krajan	1	4	110,0529	-7,5781	33	450	130

No	Time			Location					Coordinate		Slope	Length	Width
	Year	Month	Day	Subdistrict	Village	Hamlet	RT	RW	X	Y			
119	2012	January	1	Bener	Sokowuwuh	Meranti	1	1	110,0482	-7,5725	22	20	7
120	2012	January	1	Bener	Sokowuwuh		0	0	110,0423	-7,5832	30	24	9
121	2012	January	1	Bener	Sokowuwuh		0	0	110,0542	-7,5912	24	65	21
122	2012	January	1	Bener	Sokowuwuh	Krajan	1	3	110,0526	-7,5782	31	7	5
123	2012	January	1	Bener	Sokowuwuh	Balimangu	0	0	110,0448	-7,5719	16	130	89
124	2012	January	1	Bener	Sokowuwuh	Balimangu	2	2	110,0451	-7,5702	31	38	13
125	2012	January	1	Bener	Sokowuwuh		0	0	110,0411	-7,5714	24	75	31
126	2012	January	1	Salaman	Margoyoso		4	1	110,0775	-7,5613	33	21	9
127	2012	January	1	Salaman	Margoyoso		4	1	110,0783	-7,5617	30	57	22
128	2012	January	1	Salaman	Margoyoso	Blok Kalijaran	0	0	110,0797	-7,5649	25	45	15
129	2013	January	4	Bener	Ketosari		0	0	110,0606	-7,6094	33	7	5
130	2013	January	4	Bener	Kalijambe		1	1	110,0707	-7,5903	37	3	15
131	2012	January	5	Bener	Sokowuwuh	Balimangu	1	2	110,0409	-7,5715	20	7	4
132	2013	January	6	Bener	Wadas		1	3	110,0871	-7,6266	28	10	4
133	2013	December	20	Bener	Cacaban Lor	Sikopyah	0	0	110,0974	-7,6164	17	5	4
134	2014	January	12	Bener	Wadas	Karang	3	1	110,0750	-7,6306	24	7	5
135	2014	January	12	Bener	Wadas	Kaliancar	1	1	110,0736	-7,6339	31	6	5
136	2014	January	30	Salaman	Margoyoso	Tobong	0	0	110,0776	-7,5609	33	50	25
137	2014	November	29	Bener	Jati	Sawangan	1	2	110,0780	-7,5932	16	20	7
138	2014	November	30	Bener	Wadas		2	4	110,0785	-7,6218	36	25	5
139	2014	November	30	Bener	Wadas		1	4	110,0874	-7,6200	23	5	4
140	2014	November	30	Bener	Kalijambe	Gamblok	4	1	110,0693	-7,5932	37	8	10
141	2014	November	30	Bener	Bleber		2	2	110,0798	-7,6106	16	5	10
142	2014	November	30	Bener	Wadas		6	2	110,0812	-7,6223	31	5	4

No	Time			Location					Coordinate		Slope	Length	Width
	Year	Month	Day	Subdistrict	Village	Hamlet	RT	RW	X	Y			
143	2014	November	30	Bener	Bleber	Kebon Dalam	1	2	110,0797	-7,6099	15	4	4
144	2014	December	11	Bener	Wadas	Beran	1	4	110,0872	-7,6203	29	8	3
145	2014	December	12	Bener	Bleber	Sijugar	2	2	110,0710	-7,6145	12	10	5
146	2014	December	20	Bener	Kalijambe	Mantenan	2	5	110,0750	-7,5742	26	25	20
147	2014	December	11	Bener	Wadas	Kalimanggis	1	2	110,0787	-7,6261	18	10	5
148	2015		0	Salaman	Margoyoso	Kalisari	0	0	110,0660	-7,5634	32	60	100
149	2015	January	31	Bener	Wadas	Beran	1	4	110,0877	-7,6202	20	7	3
150	2015	February	8	Bener	Cacaban Lor	Pending	2	2	110,1056	-7,6178	37	5	3
151	2015	February	8	Bener	Cacaban Lor	Kemiri Sewu	2	3	110,1080	-7,6178	15	5	6
152	2015	February	8	Bener	Cacaban Lor	Kemiri Sewu	1	3	110,1099	-7,6177	30	8	6
153	2015	February	8	Bener	Cacaban Lor	Pending	2	2	110,1080	-7,6155	15	3	2
154	2015	February	8	Salaman	Margoyoso	Tlogosari	0	0	110,0776	-7,5701	34	23	30
155	2015	February	9	Bener	Pekacangan		1	5	110,1044	-7,6112	24	7	8
156	2015	April	1	Bener	Jati	Winong	1	6	110,0873	-7,5870	24	15	5
157	2015	April	18	Bener	Ketosari	Munggang	3	1	110,0552	-7,6011	15	8	10
158	2015	April	22	Bener	Jati	Sawangan	2	2	110,0780	-7,5934	15	15	5
159	2015	April	22	Bener	Jati	Sawangan	2	1	110,0785	-7,5937	19	10	10
160	2015	April	22	Bener	Jati	Jangkang	2	1	110,0811	-7,5982	29	8	3
161	2015	April	22	Bener	Jati	Jangkang	2	1	110,0808	-7,5989	22	8	3
162	2015	April	22	Bener	Jati	Jangkang	1	1	110,0798	-7,5987	32	8	3
163	2015	April	22	Bener	Jati	Kembangan	1	4	110,0848	-7,5904	15	10	8
164	2015	April	22	Bener	Jati	Kembangan Kidul	1	3	110,0802	-7,5922	15	8	3
165	2015	April	22	Bener	Jati	Kembangan	2	4	110,0809	-7,5908	23	10	8
166	2015	April	22	Bener	Bleber	Sijugar	1	2	110,0785	-7,6098	16	3	3

No	Time			Location					Coordinate		Slope	Length	Width
	Year	Month	Day	Subdistrict	Village	Hamlet	RT	RW	X	Y			
167	2015	April	22	Bener	Ketosari	Simpu	0	0	110,0588	-7,6071	30	5	3
168	2015	April	22	Bener	Kalijambe	Gamblok	1	1	110,0692	-7,5924	38	3	3
169	2015	April	22	Bener	Pekacangan	Sicengel	1	4	110,1005	-7,6086	17	15	8
170	2015	April	22	Bener	Pekacangan	Sicengel	2	4	110,1129	-7,6064	26	5	7
171	2015	May	1	Salaman	Margoyoso	Tlogosari	0	0	110,0772	-7,5719	11	4	3
172	2015	November	11	Bener	Wadas		1	4	110,0866	-7,6213	15	6	2
173	2015	December	15	Bener	Mayungsari	Santren	5	1	110,0877	-7,5805	11	6	10
174	2016		0	Bener	Ketosari	Gamblok	0	0	110,0620	-7,6021	34	10	15
175	2016		0	Bener	Ketosari		0	0	110,0589	-7,6099	27	3	25
176	2016		0	Bener	Kalijambe		0	0	110,0712	-7,5886	22	50	20
177	2016	March	7	Salaman	Margoyoso	Tobong	0	0	110,0822	-7,5645	12	12	10
178	2016	May	11	Salaman	Margoyoso	Kalisari	0	0	110,0722	-7,5649	22	30	7
179	2016	October	0	Bener	Wadas		0	0	110,0859	-7,6258	23	10	3
180	2016	October	0	Bener	Wadas		0	0	110,0879	-7,6257	23	15	10
181	2016	October	0	Bener	Cacaban Lor		1	1	110,0962	-7,6179	21	3	3
182	2016	October	0	Bener	Cacaban Lor	Pending	2	2	110,1063	-7,6181	11	3	2
183	2016	November	9	Bener	Mayungsari	Krajan 2	2	5	110,0957	-7,5800	18	3	10
184	2016	November	9	Bener	Mayungsari	Krajan 2	2	1	110,0959	-7,5789	32	4	20
185	2016	November	9	Bener	Mayungsari	Krajan 2	0	0	110,0946	-7,5808	17	3	15
186	2016	November	9	Bener	Mayungsari	Santren	0	0	110,0857	-7,5779	26	5	3
187	2016	November	9	Bener	Mayungsari	Santren	0	0	110,0911	-7,5705	15	5	3
188	2016	November	9	Bener	Mayungsari	Ngipik	0	0	110,0815	-7,5813	18	4	4
189	2016	November	9	Bener	Mayungsari	Ngipik	0	0	110,0902	-7,5730	17	4	3
190	2016	November	9	Bener	Mayungsari	Krajan 1	0	0	110,0918	-7,5813	22	4	4

No	Time			Location					Coordinate		Slope	Length	Width
	Year	Month	Day	Subdistrict	Village	Hamlet	RT	RW	X	Y			
191	2016	November	9	Bener	Mayungsari	Krajan 2	2	4	110,0927	-7,5801	17	3	10
192	2016	November	9	Bener	Mayungsari	Pakel	3	2	110,0982	-7,5756	36	4	5
193	2016	November	9	Bener	Mayungsari	Santren	4	1	110,0874	-7,5784	18	6	8
194	2016	November	9	Bener	Mayungsari	Santren	5	1	110,0854	-7,5808	25	20	10
195	2016	November	9	Bener	Jati	Winong	0	0	110,0879	-7,5865	32	20	5
196	2016	November	9	Bener	Jati	Siringin	0	0	110,0945	-7,5867	30	320	30
197	2016	November	9	Bener	Jati	Siringin	0	0	110,0953	-7,5870	23	7	6
198	2016	November	9	Bener	Jati	Siringin	0	0	110,0924	-7,5846	25	10	4
199	2016	November	9	Bener	Jati	Siringin	0	0	110,0925	-7,5848	24	10	4
200	2016	November	9	Bener	Jati	Siringin	0	0	110,0925	-7,5834	17	6	7
201	2016	November	9	Salaman	Margoyoso	Tlogosari	0	0	110,0780	-7,5719	22	130	30
202	2016	November	9	Bener	Mayungsari	Krajan 2	0	0	110,0983	-7,5783	32	700	40

Appendix 3. Weight of evidence script

```
//The parameter %1 refers to the name of the factor map.
// Each map should has a domain with the same name

//DELETE EXISTING RESULT FILES
//The crosstable s%1.tbt
//The attribute table %1.tbt
// Make a new attribute table

del s%1.*
del w%1.*
del %1.tbt
crtbl %1 %1

//CROSS THE FACTOR MAP WITH THE ACTIVITY MAP
// The cross table is called s%1

s%1=TableCross(%1.mpr,activity.mpr,IgnoreUndefs)
calc s%1.tbt

// Calculate one column in the cross table to indicate only the pixels with
landslides.

Tabcalc s%1 npixact=iff((activity=1),NPix,0)

// WE USE AGGREGATION FUNCTION, WITH OR WITHOUT A KEY TO
CALCULATE:
//nclass = number of pixels in the class. Sum the values from columns Npix and
group them by %1
//nslclass = number of pixels with landslides in the class. Sum the values from
columns Npixact and group them by %1
//nmap = number of pixels with landslides in the map. Sum the values from
columns Npix and don't group them
//nslide = number of pixels with landslide in the map. Sum the values from
columns Npixact and don't group them
//THE RESULTS STORED IN THE ATTRIBUTE TABLE %1

Tabcalc s%1 %1.nclass = ColumnJoinSum(s%1.tbt,Npix,%1,1)
Tabcalc s%1 %1.nslclass = ColumnJoinSum(s%1.tbt,Npixact,%1,1)
Tabcalc s%1 %1.nmap = ColumnJoinSum(s%1.tbt,Npix,,1)
Tabcalc s%1 %1.nslide = ColumnJoinSum(s%1.tbt,Npixact,,1)

// CALCULATE THE FOUR VALUES NPIX1 - NPIX4. THIS IS DONE IN
THE ATTRIBUTE TABLE
// Correct for the situation when Npix1 - Npix3 might be 0 pixels, and change it
```

```
into 1 pixel

Tabcalc %1 npix1 =IFF((nslclass>0),nslclass,1)
Tabcalc %1 npix2 = IFF((nslide-nslclass)=0,1,nslide-nslclass)
Tabcalc %1 npix3 = IFF((nclass-nslclass)=0,1,nclass-nslclass)
Tabcalc %1 npix4 = nmap-nslide-nclass+nslclass

//CALCULATE THE WEIGHTS IN THE ATTRIBUTE TABLE
Tabcalc %1 wplus {dom=value.dom; vr=-10:10:0.00001} =
LN((npix1/(npix1+npix2))/(npix3/(npix3+npix4)))
Tabcalc %1 wminus {dom=value.dom; vr=-10:10:0.000001} =
LN((npix2/(npix1+npix2))/(npix4/(npix3+npix4)))

//CALCULATE THE CONTRAST FACTOR
Tabcalc %1 Cw = wplus-wminus

//CALCULATE THE FINAL WEIGHT
//The final weight is the sum of the positive weight and the negative weights of
the other classes
Tabcalc %1 WminSum=aggsum(wminus)
Tabcalc %1 Wmap=wplus+Wminsum-Wminus

//MAKE AN ATTRIBUTE MAP OF THE FINAL WEIGHTS
w%1.mpr = MapAttribute(%1,%1.Wmap)
calc w%1.mpr
```

Appendix 4. RAMMS modelling guide

1. Set the preferences. It determines the place of working directory, map, orthophoto and DEM directory

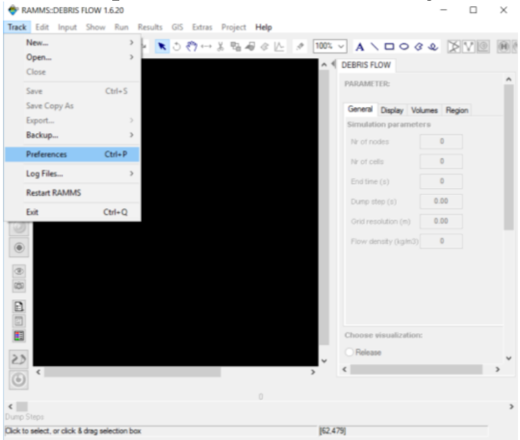

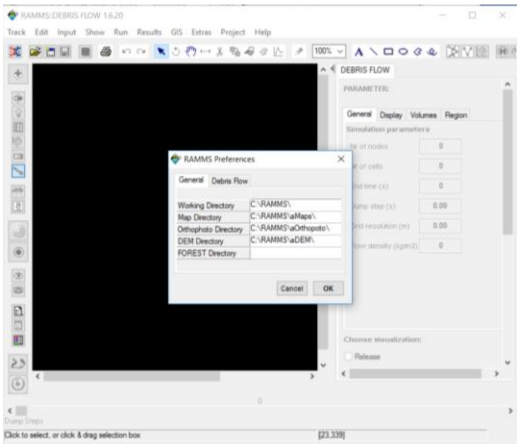

2. Start the project by clicking new project wizard under track menu. Then give the project name, set the location and import the project DEM

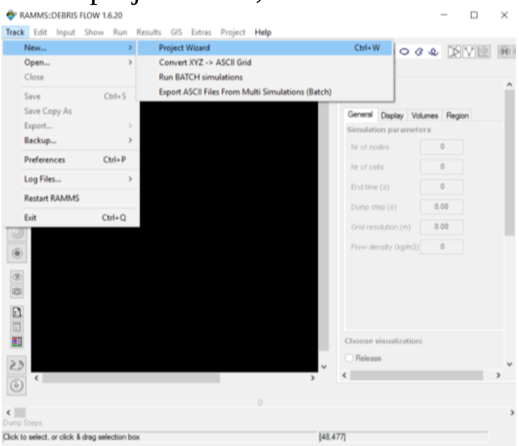

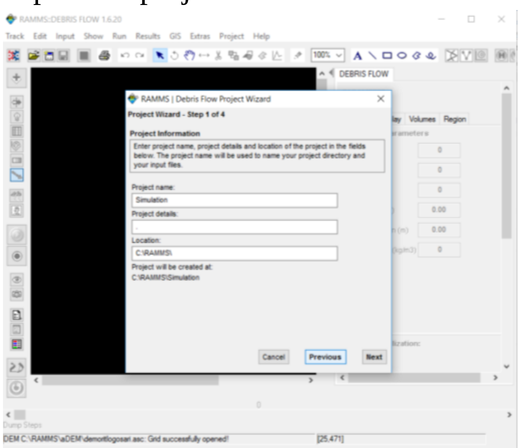

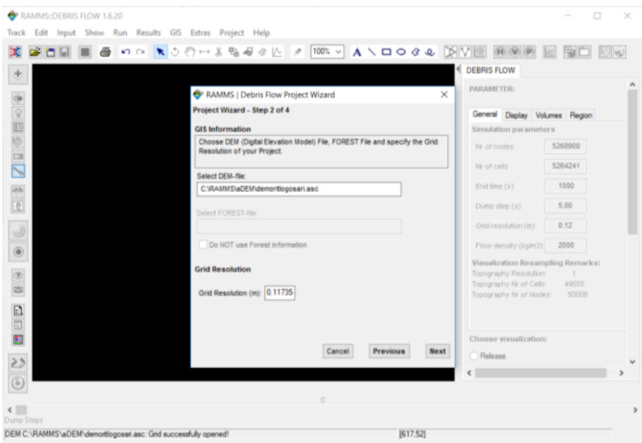

3. 3d representation will be imported.

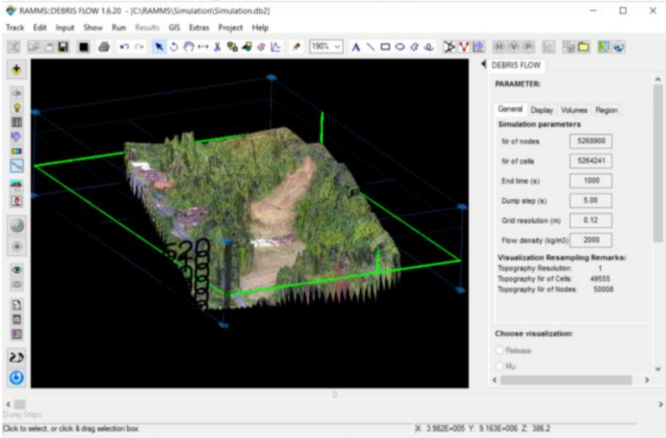

4. Create domain by switching the interface to 2d mode.

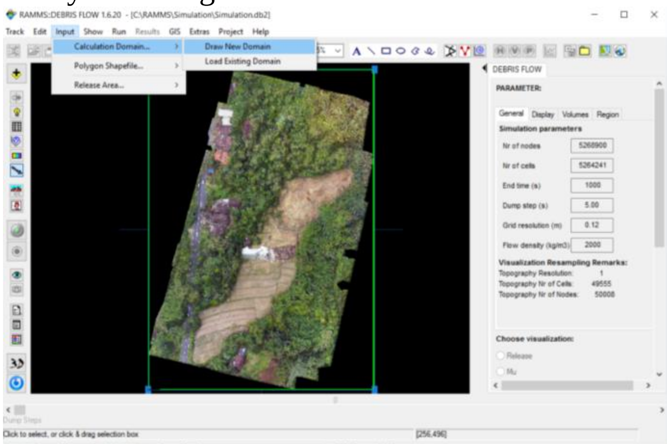

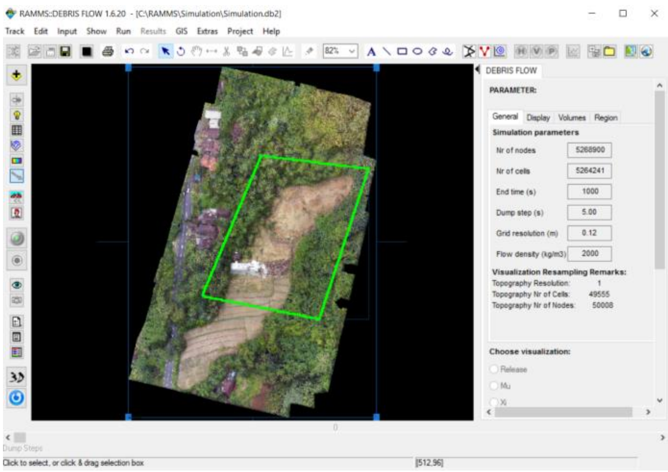

5. Create the release area and determine the release height.

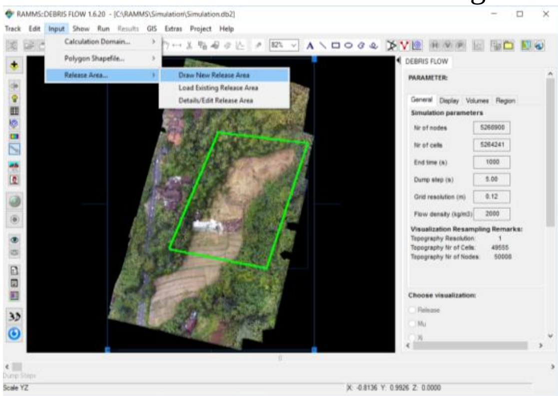

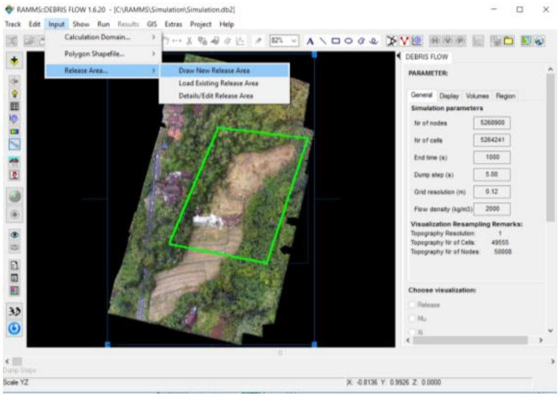

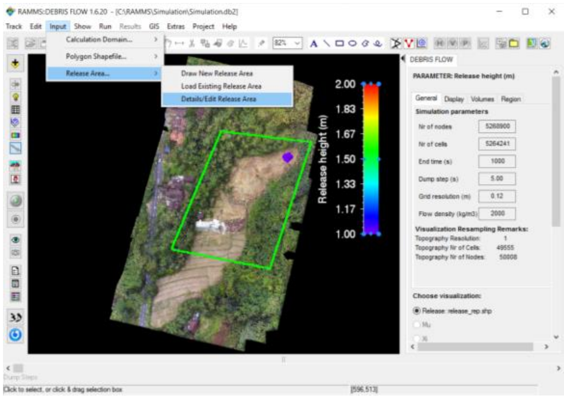

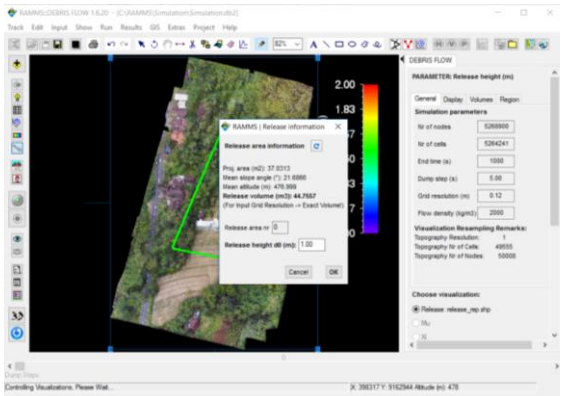

6. Strat the simulation calculation by clicking run debris flow calculation under run menu. Set simulation parameter in parameter tab, the click use block release in hydrograph tab.

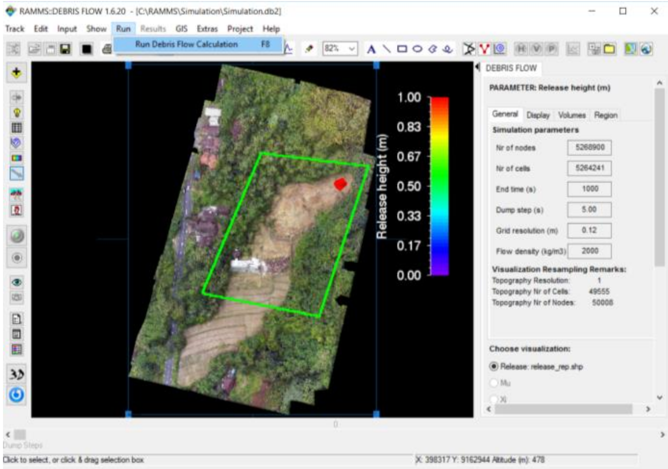

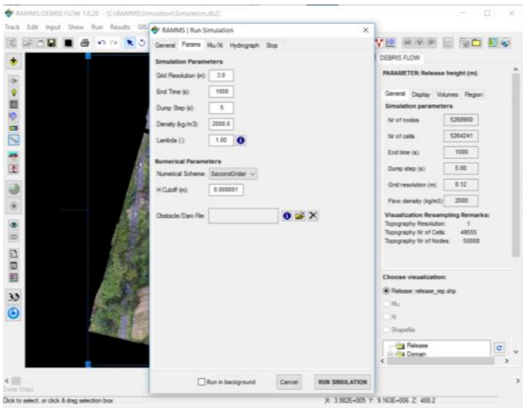

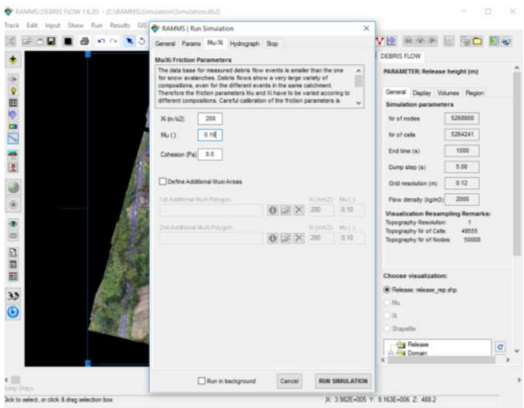

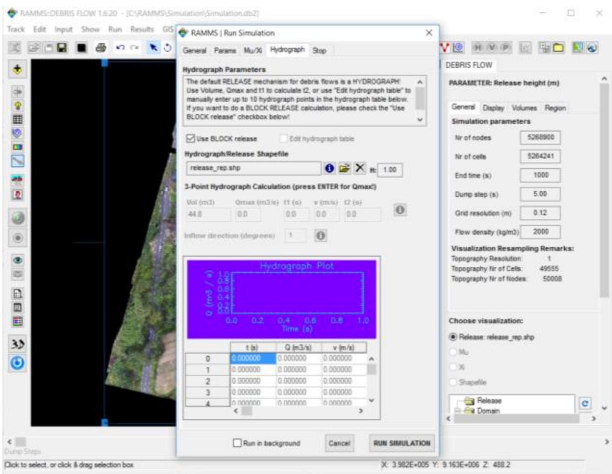

7. Calculation result will appear as well as the output log file.

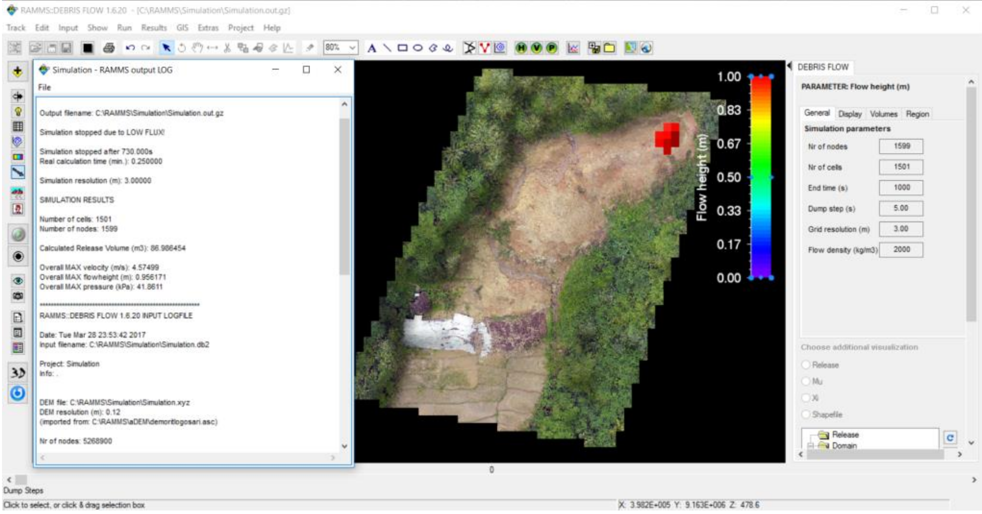

8. Simulation result can be run and visualized in different dumb step.

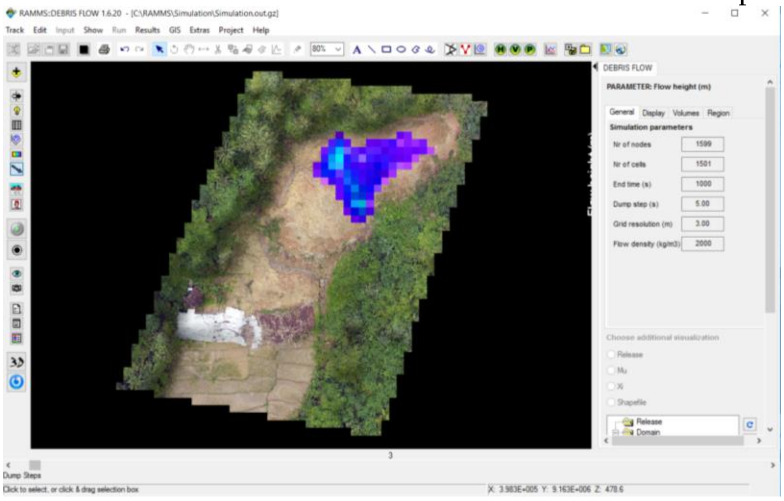

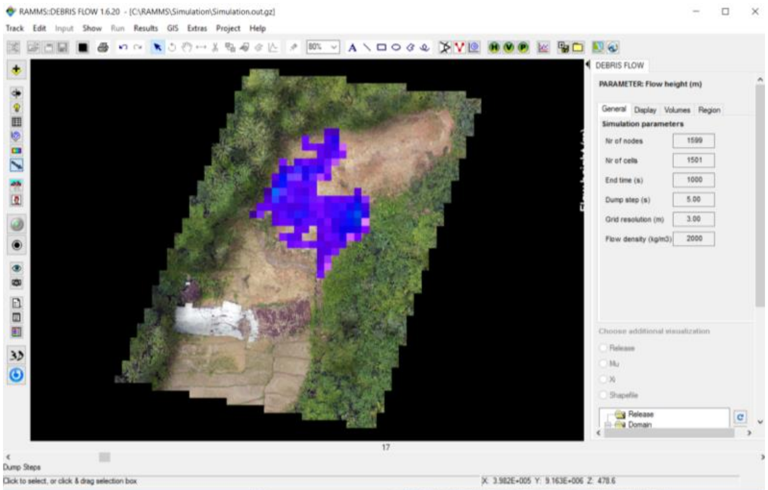

Appendix 5. Result of soil properties laboratory analysis

	Debris flows			Small landslides		
	1st	2nd	3rd	1st	2nd	3rd
USCS	SW-SM	SW	SW	MH	MH	MH
Retained on sieves no 4 (R4)	14,51 %	33,48 %	34,23 %			
Retained on sives no 200 (R 200)	93,55 %	96,02 %	97,01 %			
Finest than sives no 200 (F200)	6,46 %	3,98 %	2,99 %	> 50%	> 50%	> 50%
10% finer (D10)	0,06 mm	0,15 mm	0,12 mm			
30% finer (D30)	0,24 mm	0,74 mm	0,61 mm			
60% finer (D60)	0,96 mm	2,5 mm	2,41 mm			
Coefficient of Gradation (CG)	1,1	1,49	1,27			
Coefficient of Uniformity (CU)	17,21	17,07	19,82			
Liquid Limit (LL)	63,64			82,19	72,12	59,5
Platic Limit (PL)	41,58			49,14	41,07	37,32
Plasticity Index (PI)	22,06			33,05	31,05	22,19